



MARMARA UNIVERSITY
INSTITUTE FOR GRADUATE STUDIES
IN PURE AND APPLIED SCIENCES



PRODUCTION OF ANORTHITE FROM
INDUSTRIAL RAW MATERIALS WITH BORON
ADDITION

SİNEM YAKICI

MASTER THESIS
Department of Metallurgical and Materials
Engineering

ADVISOR
Prof. Dr. Ayhan Mergen

ISTANBUL, 2014



MARMARA UNIVERSITY
INSTITUTE FOR GRADUATE STUDIES
IN PURE AND APPLIED SCIENCES



PRODUCTION OF ANORTHITE FROM
INDUSTRIAL RAW MATERIALS WITH BORON
ADDITION

SİNEM YAKICI
(524709001)

MASTER THESIS
Department of Metallurgical and Materials Engineering

ADVISOR
Prof. Dr. Ayhan MERGEN

ACKNOWLEDGEMENT

Firstly, I would like to thank to my supervisor Prof. Dr. Ayhan MERGEN for his help during my entire study. I also would like to thank to all the members of Metallurgy and Materials Engineering Department for the help and assistance, during the entire period of my work.

April, 2014

Sinem YAKICI

CONTENT

PAGE

ACKNOWLEDGEMENT	ii
CONTENT	iii
ÖZET	iv
ABSTRACT	v
SYMBOLS.....	vi
ABBREVIATIONS.....	vii
LIST OF FIGURES.....	viii
LIST OF TABLES.....	xi
1. INTRODUCTION	1
1.1. The Aim of the Thesis.....	1
1.2. Background	3
1.2.1 Ceramic Materials.....	3
1.2.1.1. Crystalline Ceramics	3
1.2.1.2. Noncrystalline Ceramics.....	4
1.2.1.3. Electrical Properties of Ceramics	4
1.2.1.3.1. Semiconductors	4
1.2.1.3.2. Superconductivity.....	5
1.2.1.3.3. Ferroelectricity and Supersets	5
1.2.1.4. Application Areas of Ceramics.....	6
1.2.2 Substrate Materials	7
1.2.2.1. The Requirements of Substrates	8
1.2.2.2. Production Techniques of Ceramic Substrates.....	8
1.2.3. Mixed Oxide Technique	9
1.2.4. General background on Anorthite Ceramic Production	11
2. MATERIALS AND METHOD	26
2.1. Equipments and Raw Materials.....	26
2.2. Density Measurements	29
2.3. X-Ray Diffraction Analysis.....	30
2.4. Scanning Electron Microscopy Investigation	31
3. RESULTS AND DISCUSSION.....	32

3.1. Phase Analysis by XRD.....	32
3.2. Densities of Anorthite Ceramics.....	39
3.3. Microstructure Analysis Examined by SEM-EDS	42
4. CONCLUSION	57
REFERENCES	58
ÖZGEÇMİŞ	61

ÖZET

ENDÜSTRİYEL HAMMADDELERDEN BOR KATKISIYLA ANORTİT ÜRETİMİ

Bu çalışmanın amacı, düşük sinterleme sıcaklığı ve düşük üretim maliyetine sahip anortit seramiklerinin ucuz ve bol yerli hammaddelerden olan kaolen, zeolit, kalsit, wolastonit, kuvars ve bor oksit(H_3BO_3 olarak) kullanılarak üretiminin yapılmasıdır. Anortit toz karışımlarının hazırlanması için geleneksel oksitlerin karışımı yöntemi kullanılmıştır. Elde edilen tozlardan pelet üretilmiş ve bu peletler 1000-1300°C sıcaklıkları arasında 1saat boyunca sinterlenmiş ve faz gelişimleri X-ışınları difraktometresi (XRD) ve taramalı elektron mikroskobu(SEM) ile incelenmiştir. Üretilen seramiklerin yoğunlukları sinterlenme sıcaklığının fonksiyonu olarak incelenmiştir. Bor oksit ilavesinin faz gelişimi ve yoğunluğa etkisi de gözlemlenmiş, sonuçlar, başlangıç hammaddelerinin tek fazlı anortit oluşumunda faz gelişimini önemli derecede etkilediğini göstermiştir. Zeolit, kaolen ve alüminyum oksit ile birlikte CaO kullanılması, gehlenit ($Ca_2Al_2SiO_7$) ve anortit fazlarının bir arada oluşmasına neden olmuş ve 1300°C'lik sinterleme sıcaklığında bile tek fazlı anortit yapısı elde edilememiştir. Zeolit, wolastonit, alumina ve az miktarda kuvars kullanılarak hazırlanmış numunelerin 1300°C'de 1 saat sinterleme sonrası tek fazlı anortit yapısı elde edilmiştir. Fakat aynı kompozisyona ağırlıkça %3 bor oksit ilavesi anortit fazının oluşumunu hızlandırmıştır. Bunun yanı sıra wolastonit, kaolen ve alüminyum oksit kullanılan numunede yine aynı şekilde 1300°C'de tek fazlı anortit yapısı elde edilmiştir. Farklı endüstriyel hammaddelerin kullanımı 1300°C'de sinterlenen anortit seramiklerin yoğunluklarını önemli derecede etkilemiştir. Muhtemelen düşük reaktifliğinden dolayı, en düşük yoğunluk değeri CaO kullanıldığında elde edilmiş olmasına rağmen, wolastonit, kaolen ve alüminyum oksitten oluşan kompozisyon en yüksek yoğunluğu vermiştir. Borlu ve borsuz numuneler karşılaştırıldığında bor katkısının 1300°C'de yoğunluğu 92,37%'den 96,18%'e yükseldiği saptanmıştır. SEM sonuçları, XRD ve yoğunluk ölçümlerini doğrulamaktadır. EDS analizleri mikroyapıda XRD analizinde saptanan fazların dışında bir faz olmadığını göstermiştir.

Nisan, 2014

Sinem YAKICI

ABSTRACT

PRODUCTION OF ANORTHITE FROM INDUSTRIAL RAW MATERIALS WITH BORON ADDITION

The aim of this study was to produce anorthite ceramics having low sintering temperature and low production cost using cheap and abundant Turkish raw materials of kaolinite, zeolite, alumina, calcite, wollastonite, quartz, and boron oxide (as H_3BO_3). Conventional mixed oxide technique was used to prepare the anorthite ceramic powders. After mixing the starting raw materials, they were converted into pellets and sintered between 1000-1300 °C for 1h and the phase development were examined by X-ray diffraction (XRD) and scanning electron microscopy (SEM). The densities of the ceramics were examined as a function of sintering temperature. The effect of boron oxide addition on phase development and density was also investigated. The results indicated that the starting materials strongly affected the phase development during single phase anorthite formation. Usage of CaO as starting material in addition to zeolite, kaolinite and alumina gave gehlenite ($Ca_2Al_2SiO_7$) and anorthite phases and did not result in single anorthite phase formation even at 1300 °C. Employment of zeolite, wollastonite, alumina and small amount of quartz as raw materials gave single anorthite phase after firing at 1300 °C for 1h. Addition of 3wt% boron oxide into the same composition accelerated the formation of anorthite. Raw materials of wollastonite, kaolinite and alumina gave also single anorthite phase at 1300 °C. Different industrial raw materials had a considerable effect on the densities of anorthite ceramics sintered at 1300 °C. Although the lowest density was obtained when CaO was employed, possibly due to its low reactivity, raw material composition without zeolite (wollastonite, kaolinite and alumina) gave the highest density values. Comparing boron free and boron containing compositions, it can be reported that boron addition increased the density from 92, 37% to 96, 18% at 1300 °C. SEM results confirmed the XRD and density results. EDS results indicated that no any other phases were observed in the microstructure other than detected in the XRD.

April, 2014

Sinem YAKICI

SYMBOLS

T	: Temperature (°C), (°K)
t	: Time (s)
μm	: Micrometer
nm	: Nanometer
mm	: Millimeter
mL	: Milliliter
Å	: Angstrom
MPa	: Megapascal
ρ	: Density
W	: Weight

ABBREVIATIONS

BAW	: Bulk Acoustic Wave
DLS	: Dynamic Light Scattering
DSC	: Differential Scanning Calorimetry
DTA	: Differential Thermal Analysis
EDS	: Energy Dispersive Spectroscopy
FT-IR	: Fourier Transform Infrared
h	: Hour
SED	: Statistical Experimental Design Techniques
SEM	: Scanning Electron Microscopy
SAW	: Surface Acoustic Wave
TGA	: Thermogravimetric Analysis
TEM	: Transmission Electron Microscopy
XRD	: X-ray Powder Diffractometer

LIST OF FIGURES

	PAGE
Figure.1.1. Meissner Effect	5
Figure.1.2. Manufacturing processes of substrates.....	9
Figure.1.3. Mixed oxide technique flowchart.....	10
Figure.1.4. XRD patterns of the samples containing boric acid as additive.....	13
Figure.1.5. XRD patterns of the samples containing colemanite as additive	14
Figure.1.6. SEM micrographs of specimens heated at different temperatures (S11: 900°C, S12: 1100°C) and soak times (S11: 1 h, S12: 5 h)	14
Figure.1.7. The particle size (D) distributions of the Küre kaolin (KK) and Bayramiç wollastonite (BW)	16
Figure.1.8. The XRD patterns of the P2 products that were fired at different temperatures (A: anorthite, bW: b-wollastonite, Q: Quartz) (F1, F2, F3 and F4 frits were respectively labeled as P1, P2, P3 and P4).....	17
Figure.1.9. XRD traces of anorthite based porcelainised stoneware body with sintering temperature showing anorthite (A), corundum (C) and cristobalite (Q) formation	18
Figure.1.10. Typical microstructures of glass ceramics (a) D, (b) E, and (c) F made from coarse particles (10 µm), after sintering at 900 °C for 1 h. (Etching with 2 vol.% HF.).....	20
Figure.1.11. Dilatometer characteristics of the three samples studied. After attaining 1000°C, the temperature is maintained.....	22
Figure.1.12. XRD spectrum of fluorapatite–anorthite glass-ceramic at the eutectic composition	23
Figure.1.13. XRD patterns of a) boron free mixtures (BFM) and b) boron containing mixtures (BCM) sintered at different temperatures for 1 h (A=anorthite, G=gehlenite, Q=quartz, C=CaO, CS=Ca ₂ Al ₂ O ₅ , CA=Ca ₂ SiO ₄ , M=mullite).....	25
Figure 2.1. Ball mill.....	27
Figure 2.2. Flowchart of production method.....	28
Figure 2.3. Density measurement equipment	30
Figure 2.4. X-Ray Diffractometer	30
Figure 2.5. JEOL 5910LV	31

Figure 3.1. XRD pattern of S1 specimen at different temperatures	32
Figure 3.2. XRD pattern of S2 specimen at different temperatures	33
Figure 3.3. XRD pattern of S3 specimen at different temperatures	34
Figure 3.4. XRD pattern of S4 specimen at different temperatures	35
Figure 3.5. XRD pattern of all four specimens at 1000°C.....	36
Figure 3.6. XRD pattern of all four specimens at 1100°C.....	37
Figure 3.7. XRD pattern of all four specimens at 1200°C.....	38
Figure 3.8. XRD pattern of all four specimens at 1300°C.....	39
Figure 3.9. The density variation of the samples sintered at different temperatures.....	42
Figure 3.10. Secondary electron image of S1 specimen containing mainly wollastonite, zeolite, alumina and small amount of silica and heat treated at 1250°C.	43
Figure 3.11. Secondary electron image of S1 specimen containing mainly wollastonite, zeolite, alumina and small amount of silica and heat treated at 1350°C.	43
Figure 3.12. EDS analysis of S1 specimen heat treated at 1350°C (S1 contains mainly wollastonite, zeolite, alumina and small amount of silica). a) SEM micrograph showing EDS points, b) EDS analysis from anorthite phase, c) Chemical analysis of phases determined in EDS.	44
Figure 3.13. Secondary electron image of S2 specimen containing mainly wollastonite, zeolite, alumina and small amount of silica and heat treated at 1150°C.	45
Figure 3.14. EDS analysis of S2 specimen heat treated at 1150°C (S2 contains mainly wollastonite, zeolite, alumina and small amount of silica). a) SEM micrograph showing EDS points, b) EDS analysis from anorthite phase, c) EDS analysis from wollastonite phase and d) Chemical analysis of phases determined in EDS.	46
Figure 3.15. Secondary electron image of S3 specimen prepared from zeolite, kaolinite, calcium carbonate and heat treated at 1100°C.....	47
Figure 3.16. EDS analysis of S3 specimen heat treated at 1100°C (S3 contains zeolite, kaolinite, alumina and calcium carbonate). a) SEM micrograph showing EDS points, 49 b) EDS analysis from anorthite phase, c) EDS analysis from alumina phase, d) EDS analysis from wollastonite phase, e) EDS analysis from gehlenite phase and f) Chemical analysis of phases determined in EDS.....	49
Figure 3.17. Secondary electron image of S3 specimen prepared from zeolite, kaolite, calcium carbonate and heat treated at 1300°C.....	50

Figure 3.18. EDS analysis of S3 specimen heat treated at 1300°C (S3 contains zeolite, kaolinite, alumina and calcium carbonate). a) SEM micrograph showing EDS points, 51	
b) EDS analysis from anorthite phase, c) EDS analysis from alumina phase, d) EDS analysis from wollastonite phase, e) EDS analysis from gehlenite phase and f) Chemical analysis of phases determined in EDS.....	51
Figure 3.19. Secondary electron image of S4 specimen prepared from zeolite, wollastonite, alumina and small amount of silica and heat treated at 1200 °C.	52
Figure 3.20. EDS analysis of S4 specimen heat treated at 1200 °C (S4 contains zeolite, wollastonite, alumina and small amount of silica). a) SEM micrograph showing EDS points, b) EDS analysis from wollastonite phase, c) EDS analysis from anorthite phase, d) EDS analysis from alumina phase and e) Chemical analysis of phases determined in EDS.....	54
Figure 3.21. Secondary electron image of S4 specimen prepared from zeolite, wollastonite, alumina and small amount of silica and heat treated at 1350 °C.	55
Figure 3.22. EDS analysis of S4 specimen heat treated at 1350 °C (S4 contains zeolite, wollastonite, alumina and small amount of silica). a) SEM micrograph showing EDS points, b)EDS analysis from anorthite phase and c) Chemical analysis of phases determined in EDS.	56

LIST OF TABLES

	PAGE
Table1.1. Advantages and disadvantages of mixed oxide technique ^[14]	11
Table.1.2. The amounts of raw materials in the mixtures.....	12
Table 1.3. Experimental conditions of tests done in study	13
Table.1.4. The Seger formulas used in the preparation of frits and the weight percents of chemicals in the mixtures	15
Table.1.5. Chemical compositions of glass batches (wt.%)	19
Table.1.6. Mineralogical composition of raw materials and reference materials	21
Table.1.7. Ceramic paste compositions (M2 is a mix of reference materials).....	21
Table.1.8. Chemical analysis of kaolinite, calcite and quartz (%) (*Ignition loss was determined at 1100°C	23
Table.2.1. Chemical analysis of the raw materials	26
Table.2.2. Composition of samples.....	27
Table 3.1. Relative densities of the samples at different temperatures.....	40
Table 3.2. Theoretical densities of samples and raw material distribution at different temperatures.....	41

1. INTRODUCTION

1.1. The Aim of the Thesis

Anorthite that has a chemical formula of $\text{CaAl}_2\text{Si}_2\text{O}_8$ or $\text{CaO} \cdot \text{Al}_2\text{O}_3 \cdot 2\text{SiO}_2$ is also named as calcium aluminum silicate having a chemical analysis of 20.1% mass CaO, 36.7% mass Al_2O_3 , 43.2% SiO_2 . This material has a triclinic structure and can be white, gray or colorless. It is an end member and one of the rarer members of the plagioclase series. Plagioclases are framework silicates where each silica tetrahedra share all corners with its neighboring tetrahedra. It is primarily a rock-forming mineral; it is used in the manufacture of glass and ceramics.

Anorthite ceramics are promising materials for substrate applications in electronics industry due to their good physical properties. It has a thermal expansion coefficient of $45 \times 10^{-7} \text{ 1/}^\circ\text{C}$ and low dielectric constant of $\epsilon_R \approx 6.2$ at 1 MHz. This is reasonably a good match to silicon. Because of these desirable properties, anorthite ceramics have attracted great attention and several studies were carried out in order to decrease the sintering and crystallization temperature of anorthite ceramics below $1000 \text{ }^\circ\text{C}$. Low sintering temperature below $1000 \text{ }^\circ\text{C}$ is a prerequisite for substrate applications that allow the ceramic material to be co-fired with conductive metals such as copper, gold and silver.^[1]

Like most other conventional ceramics, synthesis techniques for anorthite ceramics include sintering of solid mixtures of calcium carbonate, kaolinite, alumina, and aluminum hydroxide in addition to mechanochemical treatments, sol-gel process of dehydration of appropriate metal hydroxides, or co-precipitation. All these methods carry their own advantages and disadvantages ^[1]. In addition, various additives like B_2O_3 , Na_2CO_3 , TiO_2 , CaF_2 are also used to decrease the sintering temperature or improve the properties. In this study, boric acid is used to decrease the sintering temperature.

Besides all of these advantages, the cost of anorthite is high due to the high cost of raw materials that are scarce in nature. Therefore, various studies are accomplished to produce anorthite from more abundant and cheap raw materials. Among these raw materials, one of the most promising material is zeolite which abundant and cheap.

Zeolite is a type of frame-structured hydrated aluminosilicate mineral and used abundantly as a type of natural pozzolanic material in some regions of the world^[2]. Zeolites are widely used in industry for water purification and in nuclear reprocessing due to their inherent ability to adsorb polar compounds. Their biggest use is in the production of laundry detergents. They are also used in medicine and in agriculture. Also, synthetic zeolite types are widely used as catalysts in the petrochemical industry, for instance in fluid catalytic cracking and hydro-cracking. In nuclear industry, they have uses in advanced reprocessing methods, where their micro-porous ability to capture some ions while allowing others to pass freely allow many fission products to be efficiently removed from nuclear waste and permanently trapped. In heating and refrigeration, zeolite types can be used as solar thermal collectors and for adsorption refrigeration. In these applications, their high heat of adsorption and ability to hydrate and dehydrate while maintaining structural stability is exploited. And lastly, in construction region synthetic zeolite is also being used as an additive in the production process of warm mix asphalt concrete.^[3]

Natural zeolite is an abundant raw material in many countries and having interesting ceramic properties solely through high-temperature phase transformations. Low-cost zeolitic rocks have some technological features such as low-melting temperatures, low-hardness and high-cation exchange capacity.^[4]

The greatest application potential of zeolite appears to be in gas purification, particularly trace-gas removal. Whether or not a natural zeolite is useful for a separation depends upon its adsorption characteristics for the gas components in the mixture and the particular conditions of the feed. Much can be learned by comparing the differing behaviors of well-characterized synthetic zeolites with those of natural zeolites.^[5]

In the present study, natural zeolite obtained from Bigadiç province of Balıkesir was used as the main raw material in the production of anorthite ceramic material. Besides natural zeolite, kaolinite, wollastonite, alumina and calcite were used to balance the stoichiometric composition. Boric acid was used as flux to lower the sintering temperature of anorthite.

Anorthite ceramic powders were prepared by a low cost production method of mixed oxide technique. Therefore, an introduction of this method will be given briefly.

1.2. Background

1.2.1 Ceramic Materials

A ceramic is an inorganic, nonmetallic solid prepared by the action of heat and subsequent cooling. Ceramic materials may have a crystalline or partly crystalline structure, or may be amorphous (e.g., a glass).^[6] They can be divided into two classes: traditional and advanced. Traditional ceramics include clay products, silicate glass and cement; while advanced ceramics consist of carbides (SiC), pure oxides (Al₂O₃), nitrides (Si₃N₄), non-silicate glasses and many others. Ceramics offer many advantages compared to other materials^[7]. They provide high wear, heat and corrosion resistance, as well as high tensile strength, volume resistivity, dielectric strength and modulus of elasticity. These materials also offer lower thermal expansion than metals or plastics, and a longer part life at original design dimensions and tolerances.^[8] Ceramic materials are brittle, hard, and strong in compression, weak in shearing and tension. They withstand chemical erosion that occurs in other materials subjected to acidic or caustic environments. Ceramics generally can withstand very high temperatures, such as temperatures that range from 1000 °C to 1600 °C (1800 °F to 3000 °F). A glass is often not understood as a ceramic because of its amorphous (noncrystalline) character. However, glassmaking involves several steps of the ceramic process and its mechanical properties are similar to ceramic materials.

1.2.1.1. Crystalline Ceramics

Crystalline ceramic materials are not amenable to a great range of processing. Methods for dealing with them tend to fall into one of two categories – either makes the ceramic in the desired shape, by reaction *in situ*, or by "forming" powders into the desired shape, and then sintering to form a solid body. Ceramic forming techniques include shaping by hand (sometimes including a rotation process called "throwing"), slip casting, tape casting (used for making very thin ceramic capacitors, e.g.), injection molding, dry pressing, and other variations.^[6]

1.2.1.2. Noncrystalline Ceramics

Noncrystalline ceramics, being glass, tend to be formed from melts. The glass is shaped when either fully molten, by casting, or when in a state of toffee-like viscosity, by methods such as blowing into a mold. If later heat treatments cause this glass to become partly crystalline, the resulting material is known as a glass-ceramic, widely used as cook-top and also as a glass composite material for nuclear waste disposal.^[6]

1.2.1.3. Electrical Properties of Ceramics

1.2.1.3.1. Semiconductors

Some ceramics are semiconductors. Most of these are transition metal oxides that are II-VI semiconductors, such as zinc oxide. While there are prospects of mass-producing blue LEDs from zinc oxide, ceramicists are most interested in the electrical properties that show grain boundary effects.^[9]

One of the most widely used of these is the varistor. These are devices that exhibit the property that resistance drops sharply at a certain threshold voltage. Once the voltage across the device reaches the threshold, there is a breakdown of the electrical structure in the vicinity of the grain boundaries, which results in its electrical resistance dropping from several megohms down to a few hundred ohms. The major advantage of these is that they can dissipate a lot of energy, and they self-reset – after the voltage across the device drops below the threshold, its resistance returns to being high.^[9]

This makes them ideal for surge-protection applications; as there is control over the threshold voltage and energy tolerance, they find use in all sorts of applications. The best demonstration of their ability can be found in electrical substations, where they are employed to protect the infrastructure from lightning strikes. They have rapid response, are low maintenance, and do not appreciably degrade from use, making them virtually ideal devices for this application.^[9]

Semiconducting ceramics are also employed as gas sensors. When various gases are passed over a polycrystalline ceramic, its electrical resistance changes. With tuning to the possible gas mixtures, very inexpensive devices can be produced.^[9]

1.2.1.3.2. Superconductivity



Figure.1.1. Meissner Effect

The Meissner effect demonstrated by levitating a magnet above a cuprate superconductor, which is cooled by liquid nitrogen.

Under some conditions, such as extremely low temperature, some ceramics exhibit high temperature superconductivity. The exact reason for this is not known, but there are two major families of superconducting ceramics.^[9]

1.2.1.3.3. Ferroelectricity and Supersets

Piezoelectricity, a link between electrical and mechanical response, is exhibited by a large number of ceramic materials, including the quartz used to measure time in watches and other electronics. Such devices use both properties of piezoelectric, using electricity to produce a mechanical motion (powering the device) and then using this mechanical motion to produce electricity (generating a signal). The unit of time measured is the natural interval required for electricity to be converted into mechanical energy and back again.

The piezoelectric effect is generally stronger in materials that also exhibit pyroelectricity (the ability of certain materials to generate a temporary voltage when they are heated or cooled), and all pyroelectric materials are also piezoelectric. These materials can be used to inter convert between thermal, mechanical, or electrical energy; for instance, after synthesis in a furnace, a pyroelectric crystal allowed to cool under no applied stress generally builds up a static charge of thousands of volts. Such materials are used in motion sensors, where the tiny rise in

temperature from a warm body entering the room is enough to produce a measurable voltage in the crystal.^[9]

In turn, pyroelectricity is seen most strongly in materials which also display the ferroelectric effect, in which a stable electric dipole can be oriented or reversed by applying an electrostatic field. Pyroelectricity is also a necessary consequence of ferroelectricity. This can be used to store information in ferroelectric capacitors, elements of ferroelectric RAM.^[9]

The most common such materials are lead zirconate titanate and barium titanate. Aside from the uses mentioned above, their strong piezoelectric response is exploited in the design of high-frequency loudspeakers, transducers for sonar, and actuators for atomic force and scanning tunneling microscopes.^[9]

1.2.1.4. Application Areas of Ceramics

Ceramic materials especially advanced ceramic materials are promising materials due to their high wear, heat and corrosion resistance, as well as high tensile strength, volume resistivity, dielectric strength and modulus of elasticity. With the advantage of these suitable mechanical properties are used nearly everywhere in our lives.

Traditional ceramic raw materials include clay minerals such as kaolinite, whereas more recent materials include aluminum oxide, more commonly known as alumina. The modern ceramic materials, which are classified as advanced ceramics, include silicon carbide and tungsten carbide. Both are valued for their abrasion resistance, and hence find use in applications such as the wear plates of crushing equipment in mining operations. Advanced ceramics are also used in the medicine, electrical and electronics industries.^[6] Some examples of ceramic applications depending on the industry type are listed below:

Aerospace: space shuttle tiles, thermal barriers, high temperature glass windows, fuel cells

Consumer Uses: glassware, windows, pottery, Corning™ ware, magnets, dinnerware, ceramic tiles, lenses, home electronics, microwave transducers

Automotive: catalytic converters, ceramic filters, airbag sensors, ceramic rotors, valves, spark plugs, pressure sensors, thermistors, vibration sensors, oxygen sensors, safety

passivation, encapsulation, and substrates. Considering the high temperature performance of power converters, substrates play an important role.^[11]

1.2.2.1. The Requirements of Substrates

The specific properties that should be examined when determining material suitability for a specific application are:

Thermal conductivity: The ability of a material to conduct heat away from critical circuit components. High thermal conductivity is desired.

Electrical insulation: The ability of a material to insulate various circuit components from one another. High resistance is desired.

Mechanical strength: The ability of a material to withstand mechanical shock. Young's modulus, flexural strength, tensile strength, and compressive strength are considered measures of mechanical strength. High strength is desired.

Refractory property: The ability of a material to withstand high temperatures. Melting point is an indicator of this property. This characteristic is always desirable and is absolutely mandatory for processes requiring high heat treatment (the exception being glazed-metal substrates)

Chemical susceptibility: The measure of the ability of a material to withstand exposure to chemicals. It is mandatory that substrates be inert to processing chemicals.

Weight: This may or may not be a consideration, depending on the application. It is almost always a requirement in avionic, medical, and space applications.

Metallizability: It is the ability of a material to be successfully metalized with thick, thin, or other metallization techniques.^[10]

1.2.2.2. Production Techniques of Ceramic Substrates

Substrate layers are formed by casting into sheets or tapes a blend of ceramic and glass powder, organic binder, plasticizers, and solvents. The organic components provide strength and flexibility to the green sheets during substrate personalization and fabrication.

If the ratio of ceramic to glass is high, the green substrate layer can only be sintered at firing temperatures of approximately 1500°C. Consequently, the thick-film pastes that are co-fired with the substrate layer also have to withstand these high temperatures and usually consist of refractory metals.

Raw materials for the substrate layer consist of a blend of inorganic and organic constituents. The inorganic components are various ratios of ceramic and glass powders. The organic components consist of a polymeric binder and plasticizers dissolved in a solvent.^[12]

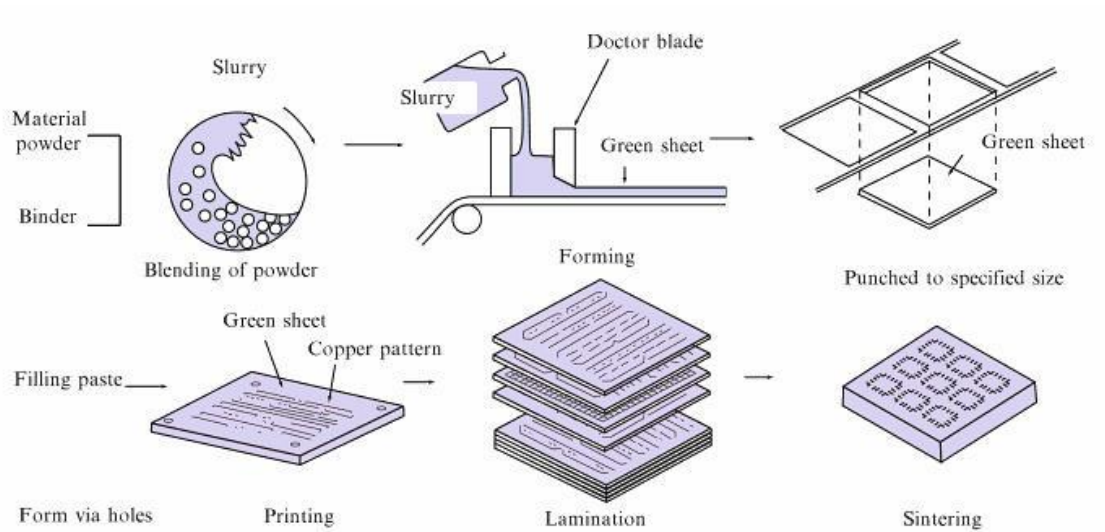


Figure.1.2. Manufacturing processes of substrates

1.2.3. Mixed Oxide Technique

The most common and easy way to obtain fine powder for piezoelectric ceramics is mixed oxide technique known also as the conventional ceramic technique. This technique is the oldest and its origins go far back in to ancient civilizations. It is simple and versatile, low cost and can be successfully applied to almost all kinds of combination of oxides. It consists of several main steps and the flow sheet presented in Fig.1.3 illustrates these steps.^[13]

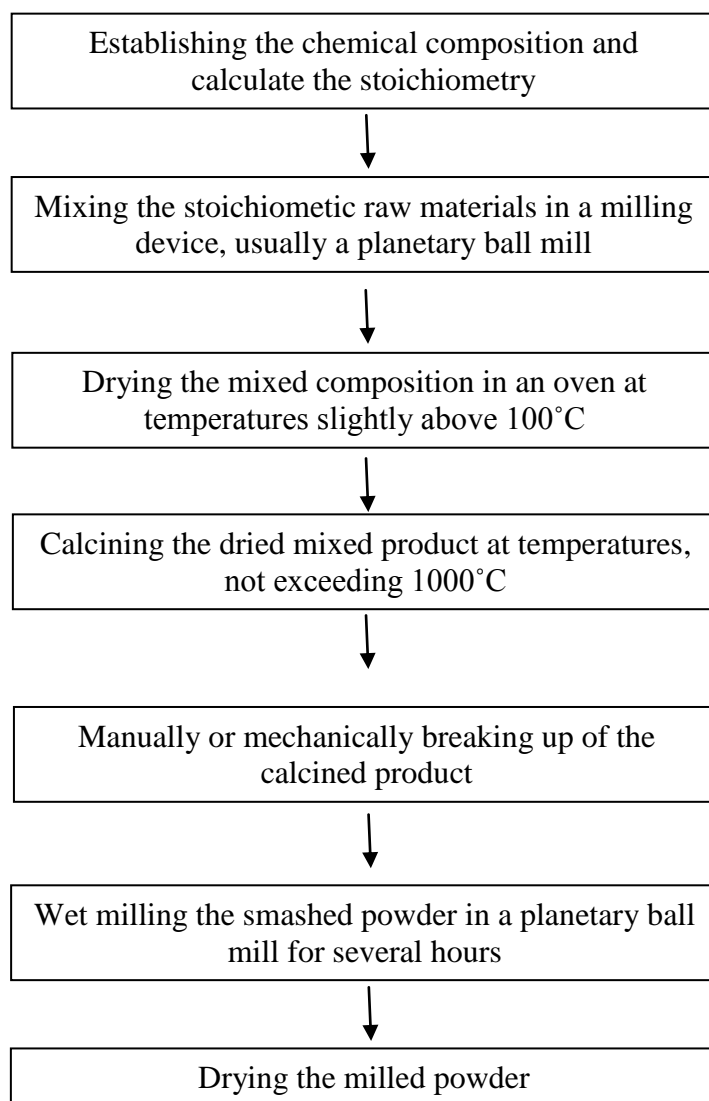


Figure.1.3. Mixed oxide technique flowchart

Mixing the raw materials is an important step in the process since the homogeneity degree of the mixture depends to a great extent on it because the amounts of each raw oxide are extremely different (varying from fraction of percent to tens of it). The mixing is generally made in a ball mill using a liquid medium such as distilled water or an organic substance such as alcohol, acetone, trichloroethylene) which do not react with no one of the raw materials.

Calcining is also important because care must be taken for a proper choice of time-temperature parameters so as to make sure that the solid state reaction between the oxides took place and the new compound was formed. The optimum time and temperature are generally found experimentally for each composition.

Milling of the calcined powder is a critical step in obtaining the fine powder required for a good ceramic. Too little milling does not produce the necessary morphologic homogeneity of the powder while an over milling may increase the likelihood of contamination with undesired atoms from jars and balls. To overcome this latter inconvenience the common practice is to use plastic lined jars with high density media such as alumina or zirconia balls. Depending of the powder composition and its characteristics as well as the mill type used, the milling time vary from several minutes to tens of hours. The particle size of the powders obtained by this technology is within the micron range or just a little under it. ^[13]

Table1.1. Advantages and disadvantages of mixed oxide technique ^[14]

Advantages	Disadvantages
Simple	Large grain size of reactants can cause slow reactions
Inexpensive method	Product can have large grain size
Wide application area	Impurities can introduce during grinding

1.2.4. General background on Anorthite Ceramic Production

Various studies have been carried out on zeolite and anorthite ceramics in the literature related to different areas like sintering kinetics, production of porcelain bodies, manufacturing of ceramic filters, and production of substrate materials for electronic industry.

As first, Kavalcı et al.^[15] studied the effects of boron addition and intensive grinding on synthesis of anorthite ceramics. Their aim was to obtain single phase anorthite ceramic with over 87% theoretical density at 950 °C using Sivas kaolinite, quartz and calcite with boric acid additions. Statistical experimental design techniques (SED) were used in order to determine and analyze the more important process variables for synthesizing anorthite ceramics. The raw materials were mixed in proper amounts to obtain a 1:1:2 stoichiometric anorthite mixture and boric acid was added as 1, 2 and 3wt% into the mixtures (Table 1.2).

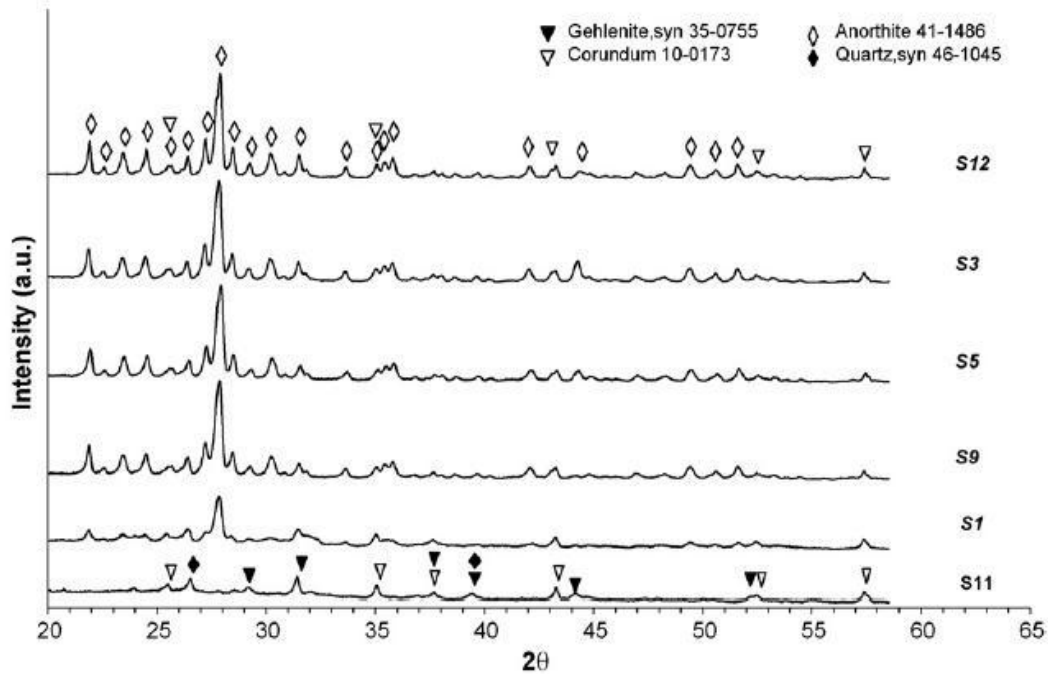
Table.1.2. The amounts of raw materials in the mixtures

The amounts of raw materials and additives for mixtures		
Raw material	Chemical formula	Amount (g)
Sivas Kaolin	$\text{Al}_2\text{O}_3 \cdot 2\text{SiO}_2 \cdot 2\text{H}_2\text{O}$	15 g
Calcium carbonate	CaCO_3	6.48 g
Alumina	Al_2O_3	1.76 g
Aluminium hydroxide	$\text{Al}(\text{OH})_3$	2.692 g
Colemanite	$2\text{CaO} \cdot 3\text{B}_2\text{O}_3 \cdot 5\text{H}_2\text{O}$	1 wt.%, 0.540 g
		3 wt.%, 1.620 g
		5 wt.%, 2.760 g
Boric acid	H_3BO_3	1 wt.%, 0.412 g
		3 wt.%, 1.236 g
		5 wt.%, 2.060 g

Phase characterizations of synthesized powders were performed by XRD using Cu K α radiation. XRD patterns for screening experiments are shown in Figs. 1.4 and 1.5 for samples containing boron oxide and colemanite, respectively. The main phase detected in samples that were fired at 1100°C was anorthite with a small amount of corundum phase such as in sample S6. Samples heated at 900°C, however, also contained other phases like gehlenite, quartz, and calcium borate in addition to the anorthite and corundum. In samples S11 and S2 the anorthite phase was not detected. The main phase in these samples was corundum with minor phases of gehlenite, calcium borate, and quartz.

Table 1.3. Experimental conditions of tests done in study

Experiment no	Additive type	Additive amount (wt. %)	Heating temperature	Soaking time	Grinding time (min)	Grinding speed (rpm)
S1	Boric acid	5	900	1h	15	500
S2	Colemanite	1	900	1h	15	100
S3	Boric acid	1	1100	5h	15	500
S4	Colemanite	1	900	5h	15	500
S5	Boric acid	5	1100	1h	15	100
S6	Colemanite	1	1100	1h	60	500
S7	Colemanite	5	1100	1h	60	500
S8	Colemanite	5	900	5h	60	100
S9	Boric acid	5	900	5h	60	500
S10	Colemanite	5	1100	5h	15	100
S11	Boric acid	1	900	1h	60	100
S12	Boric acid	1	1100	5h	60	100

**Figure.1.4.** XRD patterns of the samples containing boric acid as additive

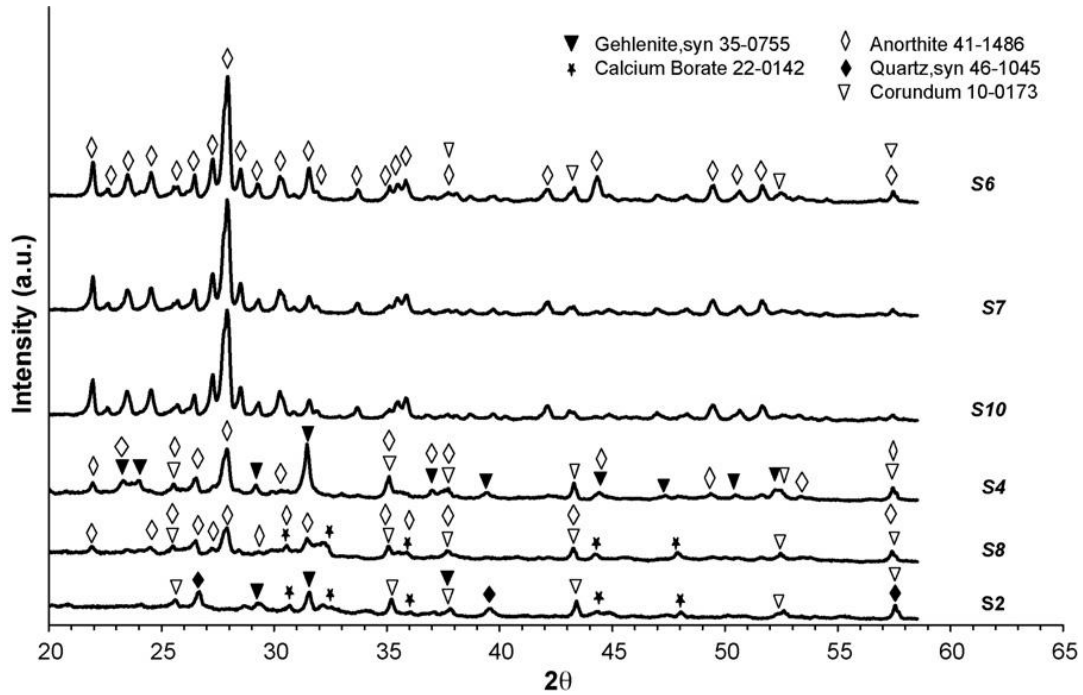


Figure.1.5. XRD patterns of the samples containing colemanite as additive

Microstructural characterization was performed by SEM. Back-scattered electron images of selected samples are presented in Fig.1.6. The sample heated at higher temperature of 1100°C was found to be denser. Phase distribution of the anorthite was found to be quite uniform in all areas of microstructure. The structure, however, had densities of around 76% of the theoretical density.

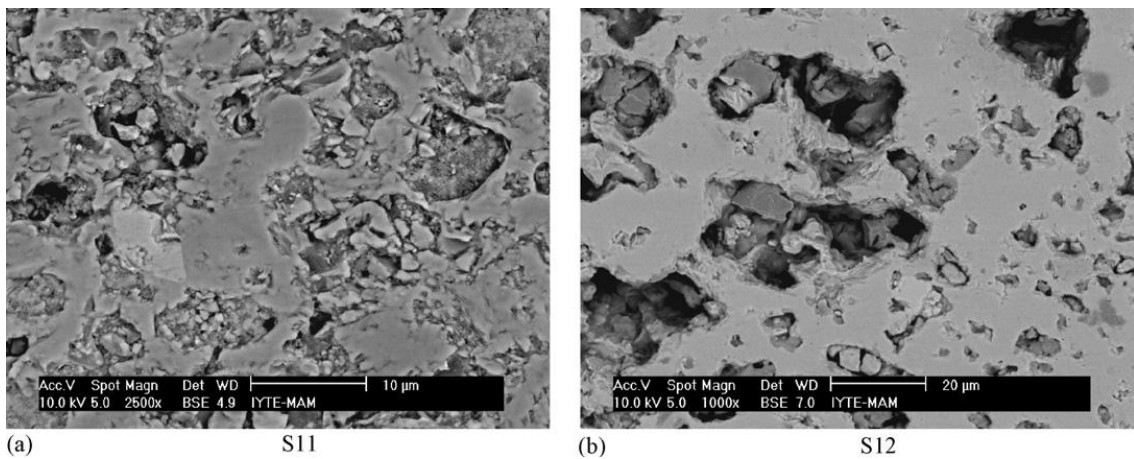


Figure.1.6. SEM micrographs of specimens heated at different temperatures (S11: 900°C, S12: 1100°C) and soak times (S11: 1 h, S12: 5 h)

The effects of different alumina sources were investigated with ladder experiments. The use of $\text{Al}(\text{OH})_3$ instead of calcined alumina as a source of Al_2O_3 slightly improved

anorthite formation. They reported that the anorthite formation temperature was decreased down to 900°C due to combined effect of additives and high speed grinding. The positive effect of high speed milling helped reduce the anorthite formation temperature. Microstructures of the heated pellets were also observed using SEM to find out that the structure was porous. Anorthite phase was successfully produced as a result of that study.

Baran et al.^[16], carried out a research about the effect of boron containing frits on the anorthite synthesis temperature using kaolinite and wollastonite as raw materials. In this research, wollastonite (CaO.SiO₂) or similar minerals were added as a source of calcium into kaolinite that is a source of aluminum and silicium. Kaolinite [Al₂Si₂O₅(OH)₄], the major clay mineral of kaolin, transforms into metakaolinite (Al₂O₃.2SiO₂) around 500 °C. Examination of the temperature-weight percent phase diagram of the wollastonite–metakaolinite system shows that the minimum temperature of anorthite formation was around 1100°C. In this study frits were added into kaolin-wollastonite mixtures, in order to decrease the anorthite formation temperatures. They have prepared four different frit compositions containing boron according to Seger formulas (Table 1.4). Also, one of these compositions included lead.

Table.1.4. The Seger formulas used in the preparation of frits and the weight percents of chemicals in the mixtures

Frit labels	Seger formulas (as mole)	Chemicals in the mixture (as mass%)
F1	1 PbO	48.3% Pb ₃ O ₄
	2 SiO ₂	25.4% SiO ₂
	1 B ₂ O ₃	26.3% H ₃ BO ₄
F2	1 NaO	32.0% SiO ₂
	3 SiO ₂	68.4% Na ₂ B ₄ O ₇ .10H ₂ O
	2 B ₂ O ₃	
F3	1 K ₂ O	31.7% SiO ₂
	3 SiO ₂	43.7% H ₃ BO ₄
	2 B ₂ O ₃	24.5% K ₂ CO ₃
F4	0.45 Na ₂ O	8.9% SiO ₂
	0.45 K ₂ O	34.2% Na ₂ B ₄ O ₇ .10H ₂ O
	0.10 CaO	7.4% K ₂ CO ₃
	0.20 Al ₂ O	41.4% KAlSi ₃ O ₈
	1.80 SiO ₂	3.4% CaSiO ₃
	0.60 B ₂ O ₃	

Researchers produced cylindrical pellets prepared from each of the batches to fire up at different temperatures. They reported that as wollastonite particles were coarser, particle size distribution curves (Fig.1.7) were rather close to each other.

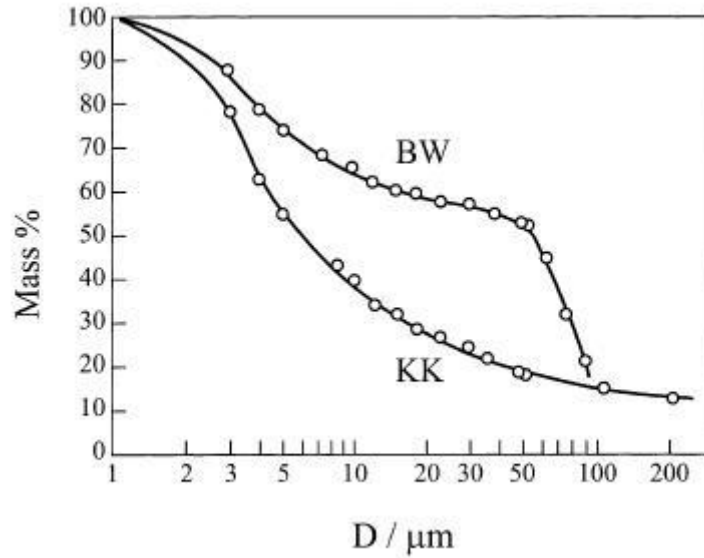


Figure.1.7. The particle size (D) distributions of the Küre kaolin (KK) and Bayramiç wollastonite (BW)

In addition, X-ray diffraction (XRD) patterns of the sintered ceramics indicated that the minimum anorthite formation temperature was 1000 °C (Fig.1.8). However, it was determined that leaded and unleaded boron containing frits decreased the anorthite formation temperature from 1100 to 1000°C in kaolin-wollastonite mixture. It was observed that introduction of lead into the frit composition had no favorable effect towards a decrease in anorthite formation temperature. This observation is favorable considering the possible disadvantages of lead such as toxicity in porcelain batches. A decrease of 100 °C in anorthite formation temperature is prone to lead to considerable energy economy in single firing porcelain production.

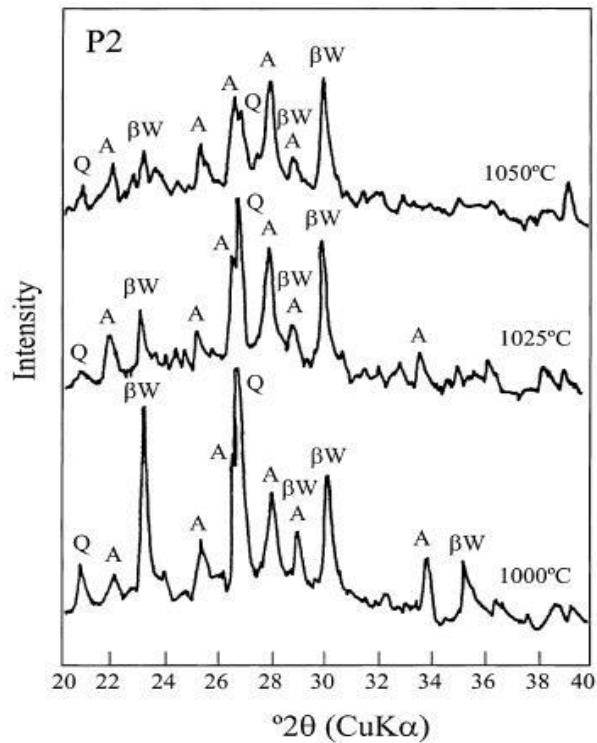


Figure.1.8. The XRD patterns of the P2 products that were fired at different temperatures (A: anorthite, βW : b-wollastonite, Q: Quartz) (F1, F2, F3 and F4 frits were respectively labeled as P1, P2, P3 and P4)

Capoglu et al.^[17] carried out a study that aimed to design and develop an alternative composition for making porcelainised stoneware, having better properties than the conventional porcelainised stonewares. Contrary to the conventional porcelainised stonewares, that new composition is designed to develop basically anorthite ($\text{CaO}\cdot\text{Al}_2\text{O}_3\cdot 2\text{SiO}_2$) crystals in the microstructure and to have a high crystalline to glassy phase ratio, after processing at 1200–1225 °C temperature ranges. In order to produce anorthite crystals, wollastonite, calcined alumina, quartz, Ukrainian Ball Clay and some magnesia were used as raw materials. Technological properties, such as density, water absorption, firing shrinkage, flexural strength, thermal expansion behavior and aesthetical properties were measured. X-ray diffraction (XRD) and scanning electron microscopy (SEM) studies were also carried out to analyze the microstructure.

The density of the anorthite-based ceramics was studied in the temperature range from 1150 to 1300°C with 25°C intervals to explore the densification behavior of the ceramics. It was found that as the sintering temperature increased, bulk density and

firing shrinkage of the body continued to increase and reached a maximum at around 1200 °C and then decreased. The XRD analysis (Fig.1.9) demonstrated that the crystalline phases identified in all the specimens fired in the temperature range from 1150 to 1250°C are anorthite being the major phase, cristobalite and corundum. While the peak intensity of anorthite increased significantly with the increase of sintering temperature, peak heights for corundum and cristobalite decreased. This indicated that the increase of sintering temperature decreased the content of free cristobalite and corundum. The maximum flexural strength was obtained with the anorthite based porcelainised stoneware was about 110MPa which is much higher than that of commercial stoneware products (55MPa). A new material from a mixture of wollastonite, alumina, quartz, magnesia and Ukrainian Ball Clay was produced in order to meet the porcelainised stoneware requirements. It was reported that it was possible to densify the ceramic material in the temperature ranges between 1200–1230 °C. The properties of the porcelainised stonewares such as whiteness, water absorption, thermal expansion coefficient and the flexural strength were significantly better than the conventional porcelainised stoneware. Without modifying the process and technological conditions of the present industry substantially the new material could be manufactured. Therefore, it is an excellent candidate material for the stoneware industry.

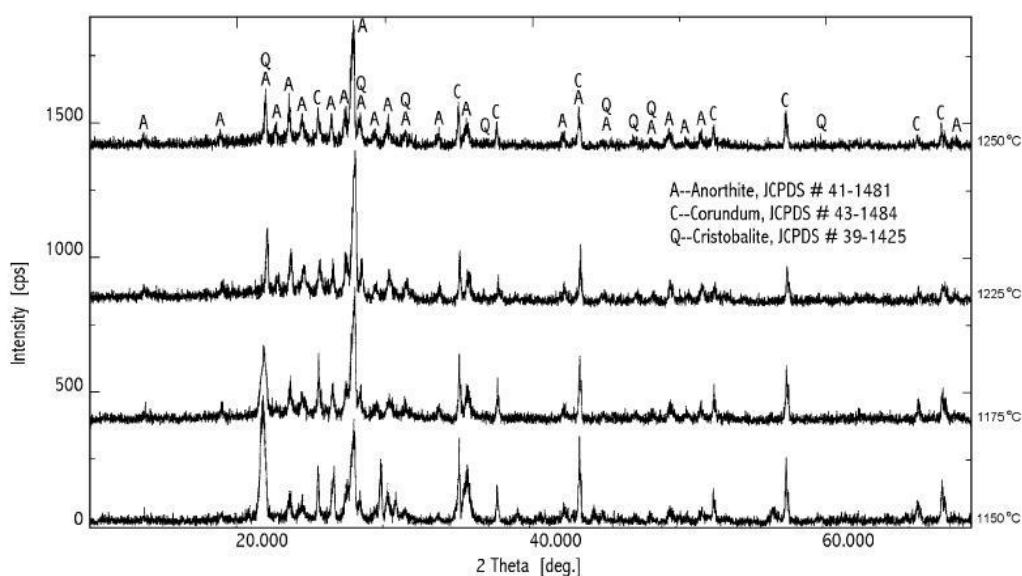


Figure.1.9. XRD traces of anorthite based porcelainised stoneware body with sintering temperature showing anorthite (A), corundum (C) and cristobalite (Q) formation

Ferreira et al.^[18] made a study on low temperature production of glass ceramics in the anorthite–diopside system via sintering and crystallization of glass powder compacts (Table 1.5). To investigate the influence of particle size of glass powders on the properties of glass ceramics the milling conditions were adjusted in a way to produce a group of fine powders (mean particle size 2 μm) and a group of coarse powders (ca. 10 μm). Rectangular bars (4 mm x5mm x50 mm) of glass powder compacts were produced by uniaxial pressing (80 MPa) using fine and coarse powders to compare the effect of fine and coarse powders on mechanical properties. The bars were heat-treated in air at different temperatures of 800, 825, 850, 900, and 950° C for 1 h with heating and cooling rates of 5 °C/min.

Table.1.5. Chemical compositions of glass batches (wt.%)

Chemical compositions of glass batches (wt.%)							
Composition	SiO ₂	Al ₂ O ₃	CaO	MgO	P ₂ O ₅	CaF ₂	B ₂ O ₃
D	44.91	20.52	23.32	6.95	1.98	0.36	1.96
E	46.50	17.28	24.09	8.77	2.00	0.37	0.99
F	47.57	15.69	24.60	9.75	2.02	0.37	–

The investigated glasses were successfully melted at the chosen melting conditions. Their casting ability was also very good. After quenching in cold water, the resultant frits were bubble-free, transparent, and colorless. X-ray diffraction analysis of frits showed their absolute vitreous state and the absence of devitrification. Microstructure observations were carried out on fracture surfaces by scanning electron microscopy.

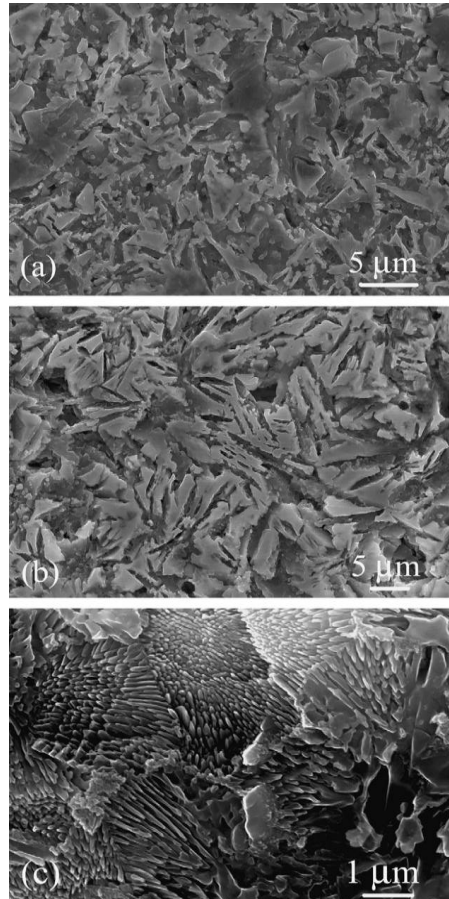


Figure.1.10. Typical microstructures of glass ceramics (a) D, (b) E, and (c) F made from coarse particles (10 μm), after sintering at 900 $^{\circ}\text{C}$ for 1 h. (Etching with 2 vol.% HF.)

They attained some results at the end of their experiments that anorthite–diopside glass ceramic can be produced at relatively low temperatures (850–900 $^{\circ}\text{C}$) via sintering and crystallization of glass powder compacts. The highest values of density and shrinkage along with zero water absorption were obtained at 825 $^{\circ}\text{C}$ for the samples made of fine powders and at 850 $^{\circ}\text{C}$ for the samples made of coarse powders. They reported that increasing the anorthite portion in the glass caused a shift in T_g and crystallization peaks to higher temperatures, which may be attributed to the role of Al^{3+} as a network former in the structure of the glasses. They also experienced that there was a direct relation between particle size and mechanical strength that the particle size of the powders influences the quality of the produced glass-ceramics. When using fine powders than coarser ones, densification and crystallization occurred at lower

temperatures. The use of coarse particles had positive effect on density and mechanical properties.

Blanchart et al.^[19] made a study to decrease the sintering temperature of pottery clay and to improve the mechanical properties of fired pottery products, using calcite as an additive, taking into account the traditional practices of potteries. To study the thermal behavior of a raw material, a common practice was to consider the behaviour of a raw material in terms of an ideal formula of a pure mineral mix presenting well-known chemical compositions and structural characteristics. They used kg2 as a reference material (Table 1.6).

Table.1.6. Mineralogical composition of raw materials and reference materials

Sample (wt.% dry mass)	Kaolinite	Quartz	Calcite	Organic matter and other minerals
P1	71.4±1	21.1±1	0	7.5±1
P2	60.7±1	17.9±1	15.0±1	6.4±1
Kg2	>93	-	-	<7

Table.1.7. Ceramic paste compositions (M2 is a mix of reference materials)

Ceramic paste compositions

Ceramic paste (wt.% dry mass)	P1	Kg2	Quartz	Calcite
P1	100	0	0	0
P2	85	0	0	15
M2	0	64.2	20.8	15

The dilatometric curves of the three compositions (Fig.1.11) as a function of time are given. They discovered that When the sintering temperature is reached and maintained at 1000°C, a progressive densification for 15 min and subsequent volume stabilization (even after long dwell times) was observed Finally, P2 is more densified than P1 and M2 is the most highly densified composition (Table 1.7). They revealed that anorthite was the most important phase formed during the sintering. At the low firing temperature, it appears that the firing process was characterized by the absence of a liquid phase, drastically limiting the diffusion effect. The sample microstructure, as observed by SEM, showed a network of small dense zones, including quartz grains,

interconnected by recrystallized porous phases. The comparison of material containing the natural kaolinitic clay to material obtained from pure reference minerals underlined the important role of iron impurities. The strength of the material appears to be related to the type and quantity of crystalline phases rather than to a decrease of porosity. Ca-rich regions form a connecting network between more highly densified zones where larger quartz grains remain. Furthermore, the use of reference minerals revealed the particular role of raw material impurities, which reduce crystalline phase formation.

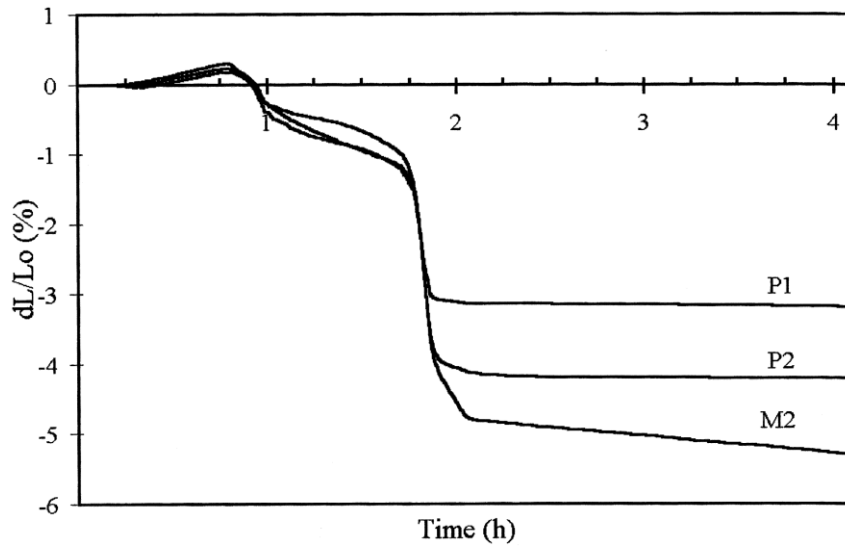


Figure.1.11. Dilatometer characteristics of the three samples studied. After attaining 1000°C, the temperature is maintained

Correia et al.^[20] performed a study related with the fluorapatite–anorthite system in biomedical application. Glass blocks were prepared using reagent-grade SiO₂, Al₂O₃, CaCO₃, (NH₄)₂HPO₄ and CaF₂ powders. Properly mixed batches of the initial components were pre-heated at 900°C for 6–8 h in order to avoid P₂O₅ volatilization. The mixtures were then melted in alumina crucibles in air, at 1500°C (i.e. B1201 above liquidus temperature) for 2 h to ensure homogeneity. The melts were cast into a ribbed bar and, once removed from the mould; glasses underwent annealing at 650–700°C for 1–2 h. XRD examination revealed that fluorapatite and anorthite were exclusively identified, (Fig.1.12). A high degree of crystallization can be observed, while a small amount of a glassy phase is also suggested. As a result of their experiences, the system of fluorapatite-anorthite exhibits biocompatibility in terms of bioacceptability and absence of any irritation or toxicity effects in the in vivo tests, while no dissolution of

toxic Al^{3+} ions was detected at all in the in vitro tests. The glass-ceramic exhibits high chemical stability in biological environment and therefore can be classified as inert biomaterial.

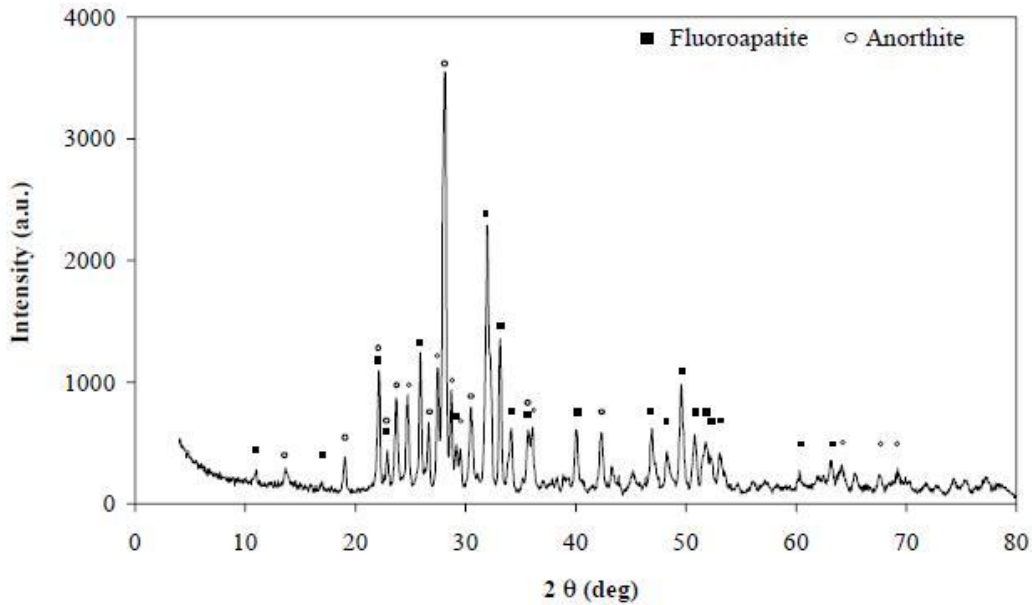


Figure.1.12. XRD spectrum of fluorapatite–anorthite glass-ceramic at the eutectic composition

Gürü et al.^[21] carried out an study about production of anorthite ($\text{CaO} \cdot \text{Al}_2\text{O}_3 \cdot 2\text{SiO}_2$) from kaolinite and CaCO_3 via colemanite (Table 1.8). Inexpensive starting materials of kaolinite, calcium carbonate and silica were used for anorthite ceramic production. Boron oxide was used as sintering aid due to its low melting point and less harmful effect on the insulating characteristics than the other sintering aids. 3 wt% boron oxide (B_2O_3) was added into the mixture as colemanite ($2\text{CaO} \cdot 3\text{B}_2\text{O}_3 \cdot 5\text{H}_2\text{O}$) and the effects of colemanite upon the transformation towards anorthite and on the densification were investigated between 900-1400 °C. Boron oxide has been found to be useful flux for the preparation of dense anorthite ceramics. Single phase anorthite ceramic formed at lower temperatures in boron containing mixtures. Boron containing powder compacts were sintered above 90% theoretical density at 1350 °C.

Table.1.8. Chemical analysis of kaolinite, calcite and quartz (%) (*Ignition loss was determined at 1100°C

	SiO ₂	Al ₂ O ₃	TiO ₂	Fe ₂ O ₃	CaO	MgO	Na ₂ O	K ₂ O	LOI*
Kaolinite	43.85	38.03	0.08	0.83	0.26	0.08	0.12	0.22	16.08
Calcite	0.09	0.1	0.01	0.02	54.67	1.74	0.06	0.01	43.20
Quartz	99.21	0.15	0.04	0.07	0.06	0.03	0.01	0.05	0.16

Starting materials were wet mixed in deionised water for 5 h using alumina balls in a plastic container. In order to compare the results, anorthite powders were also produced without colemanite addition using the same raw materials (BFM). After drying, the powders were pressed into pellets of 25 mm diameter with a pressure of 80 MPa. The green compacts were fired in air in the range 900-1400 °C for 1 h with a heating and cooling rate of 300 °C/h. The phases present in the samples were analyzed by X-ray diffractometer (Siemens) using CuK α .

XRD patterns of the sintered ceramics suggested that boron oxide addition as colemanite accelerated the formation and densification of anorthite produced from kaolinite, calcite and quartz with relatively coarse particles (Fig.1.13). Although single anorthite phase ceramic was obtained at 1200 °C by boron oxide incorporation, boron free specimens gave only single anorthite phase at 1300 °C. A relative density of 91.3% was obtained from boron containing mixtures at 1350 °C whereas boron free specimens had a relative density of 73.5% even after sintering at 1350 °C for 1 h.

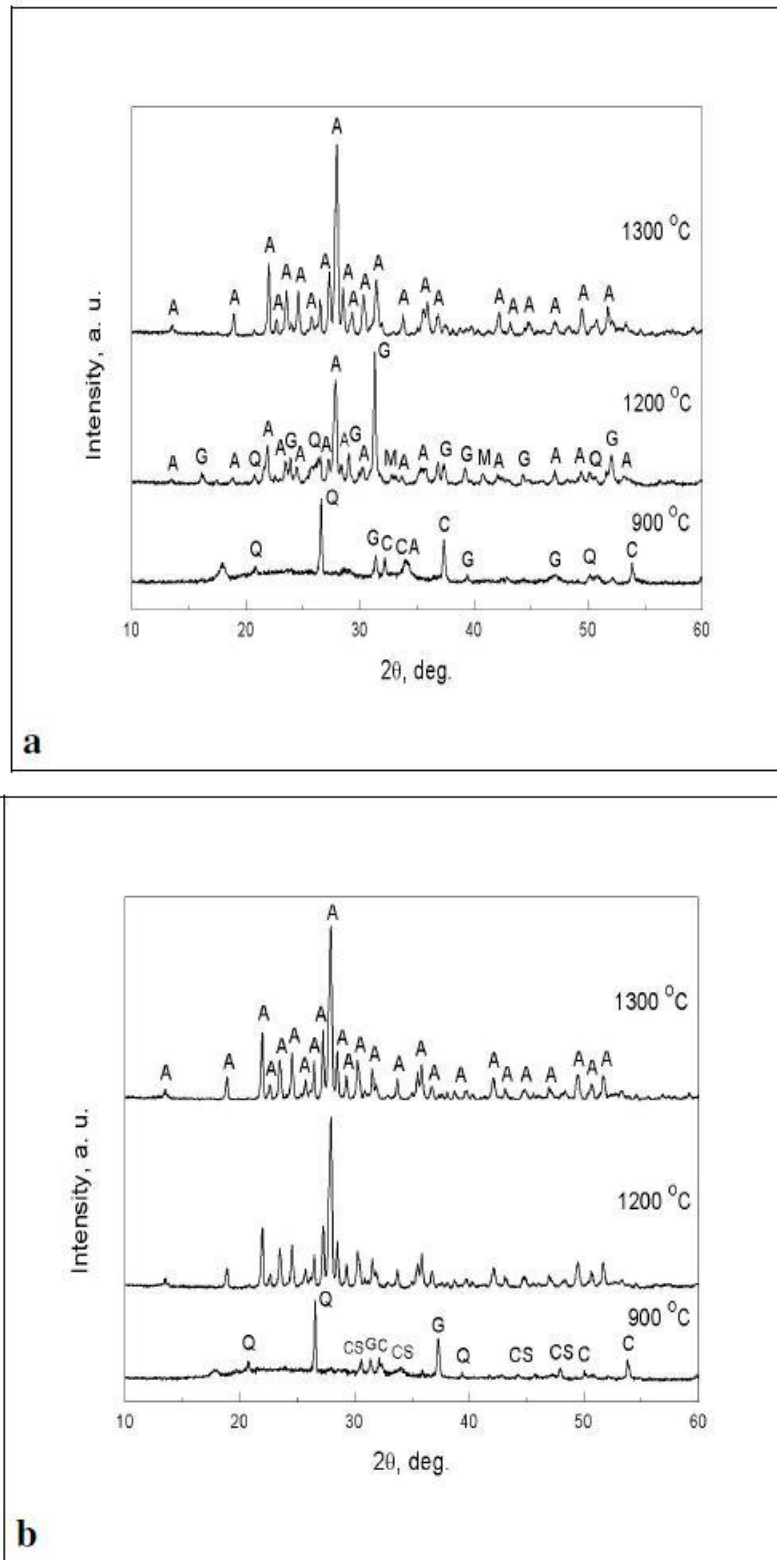


Figure.1.13. XRD patterns of a) boron free mixtures (BFM) and b) boron containing mixtures (BCM) sintered at different temperatures for 1 h (A=anorthite, G=gehlenite, Q=quartz, C=CaO, CS=Ca₂Al₂O₅, CA=Ca₂SiO₄, M=mullite)

2. MATERIALS AND METHOD

2.1. Equipments and Raw Materials

Anorthite ceramics were produced by conventional ceramic production technique of mixed oxide and the densities, sintering behavior and microstructures of anorthite ceramics were examined and the produced powders and ceramics were characterized in detail.

The starting ceramic raw materials kaolinite ($\text{Al}_2\text{Si}_2\text{O}_5(\text{OH})_4$), zeolite ($((\text{Ca},\text{K}_2,\text{Na}_2,\text{Mg})_4\text{Al}_8\text{Si}_{40}\text{O}_{96}\cdot 24\text{H}_2\text{O})$), calcite (CaCO_3), alumina (Al_2O_3), wollastonite (CaSiO_3) and quartz (SiO_2) were supplied from Eczacıbaşı Esan, Turkey. Boric acid was supplied from Eti Mine Works General Management. Chemical analyses of the raw materials are given in Table 2.1.

Table.2.1. Chemical analysis of the raw materials

	Zeolite	Kaolinite	Wollastonite	Alumina	Quartz	Boric acid
SiO₂	67.74	49.00	53.00	0.02	99.30	00.00
CaO	3.71	0.06	44.00	0.01	0.03	00.00
Al₂O₃	11.28	36.00	00.00	99.00	0.30	00.00
Fe₂O₃	1.51	0.75	0.19	0.025	0.03	00.00
MgO	2.02	0.30	00.00	00.00	0.02	00.00
Na₂O	0.25	0.10	00.00	0.50	0.15	00.00
K₂O	3.10	1.85	00.00	00.00	0.04	00.00
TiO₂	0.21	0.02	00.00	00.00	00.00	00.00
B₂O₃	00.00	00.00	00.00	00.00	00.00	56.25

In this study, four main batches were prepared with different composition mixtures to produce anorthite compositions. They are formulated so as to correspond to the stoichiometric composition of anorthite phase (CaO 20,14%, Al₂O₃ 36,68% and SiO₂ 43,18%). In order to observe the effect of the addition of boron oxide on anorthite formation and on densification, one batch was set with 3wt% boron oxide addition. Boron oxide was added as boric acid (H₃BO₃) which was used as sintering aid due to its low melting point and less harmful effect on the insulating characteristics than the other sintering aids. The weight percentage of each batch is given in the Table 2.2. S1 and S3

batches were designed to contain mainly zeolite and the other deficient oxides were added as wollastonite, kaolinite, alumina, quartz and calcium carbonate. Although in S1 deficient CaO, Al₂O₃ and SiO₂ were supplied from wollastonite, alumina and quartz, in S3 they were supplied from calcium carbonate, kaolinite and alumina. S1 and S4 batches were same and the only difference S4 contained 3wt% boron oxide but S1 did not include boron oxide. S2 batch did not contain zeolite but it included wollastonite, kaolinite and alumina.

Table.2.2.Composition of samples

wt%	Zeolite	Wollastonite	Kaolinite	Alumina	Quartz	Calcium carbonate	Boric acid
S1	26,37	40,45	0,00	32,15	1,03	0,00	0,00
S2	0,00	42,18	37,19	20,63	0,00	0,00	0,00
S3	18,80	0,00	36,76	10,69	0,00	33,75	0,00
S4	25,13	38,54	0,00	30,64	0,98	0,00	4,71

Stoichiometric powders were wet mixed and milled in ethyl alcohol using zirconia balls in a plastic container for 10 h in a ball mill (Fig.2.1). Following the mixing, the mixtures were dried at 90°C for 24 h. After drying, the mixtures were homogenized in an agate mortar and uniaxially pressed at 100 MPa into pellets approximately 10 mm in diameter and 1-2 mm in thickness. The green compacts were sintered in an electrically heated furnace (Nabertherm) in air between 1000-1300°C for 1 h with a heating and cooling rate of 300 °C/h. The general flow diagram of the production method is given in Fig.2.2.



Figure 2.1. Ball mill

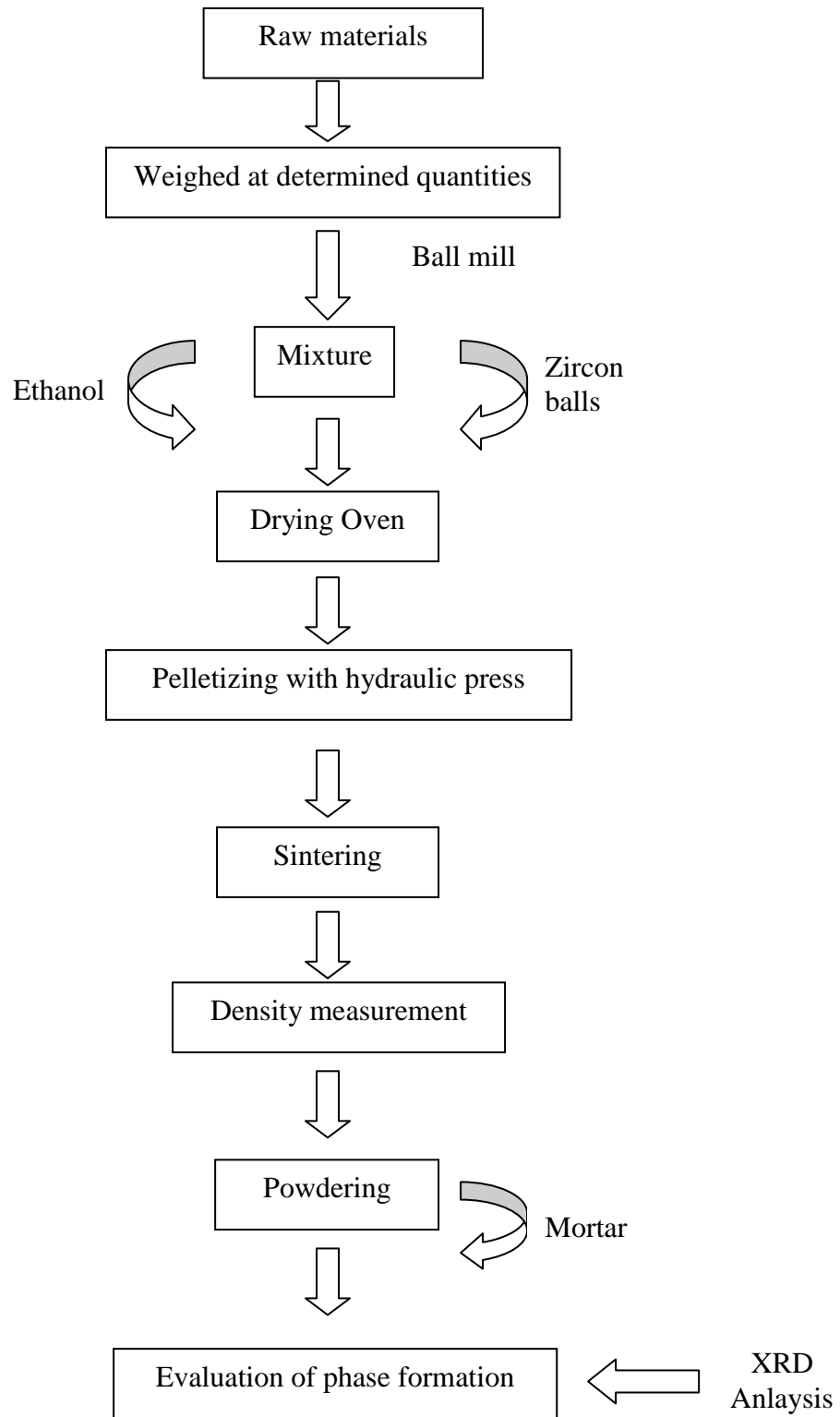


Figure 2.2. Flowchart of production method

2.2. Density Measurements

After sintering, the densities of the samples were measured by Archimedes method (Fig.2.3). To increase the accuracy of the measurement, the pellets were ground using 800 and 1200 grade SiC paper and two specimens were prepared for each firing temperature and each specimen measured twice and the average was taken as final result. The diameters and thicknesses of the sintered pellet were measured by a digital caliper (Mitutoyo). Measuring the density of the pellets involved several steps. Initially, the weight of the pellet was measured (W_a), then they were immersed into the deionized water and boiled for a short while. The pellets were taken out from the water and the surfaces of the pellets were gently cleaned. The wet weights of the pellets were recorded (W_b). Following these measurements, the bulk density of the pellets (ρ_b) can be calculated from the following equation:

$$\text{Bulk Density } \rho_b = \frac{W_a}{W_b} \times \rho_{su} \quad (2.1)$$

$$\text{Relative density } \rho_{RD} = \frac{\rho_b}{\rho_{teorik}} \times 100 \quad (2.2)$$

W_a = Dry mass of the sample,

W_b = W_{wet} - $W_{in\ water}$,

ρ_b = volume density,

ρ_{RD} = relative density,

ρ_{su} = water density,

$\rho_{theoretical}$ = theoretical density of the sample.



Figure 2.3. Density measurement equipment

2.3. X-Ray Diffraction Analysis

Sintered pellets were ground into powder in an agate mortar for phase analysis using X-ray diffractometer (Rigaku X-ray Diffractometer) (Fig.2.5). Analysis were done to examine the phase development depending on sintering temperature and to determine the second phases. The powdered samples were prepared by placing on glass sample holders. XRD analysis was performed by using Ni filtered Cu $K\alpha$ radiation, in the range of $5-70^\circ$ with $1^\circ/\text{min}$ scanning rate. XRD results were analyzed using MDI Jade6.5 software program.



Figure 2.4. X-Ray Diffractometer

2.4. Scanning Electron Microscopy Investigation

The microstructure of sintered samples was investigated using Scanning Electron Microscopy (SEM). Fracture surfaces of the samples were examined by breaking the pellets into two. After fixing the sintered samples on aluminum sample holders with carbon types, in order to increase surface conductivity for SEM analysis, they were coated with Au alloy. This coating process was done with 4mA current and 3-5 minutes long by using Polaron Range Sputter Coater-SC7620. JEOL 5910-LV Scanning Electron Microscope equipped with Oxford-Inca-7274 Energy Dispersive Spectrometer (Fig.2.6) was used for examination of fracture surfaces of sintered pellets. EDS was used for compositional analysis of phases, where secondary electron imaging (SEI) and backscattered electron imaging (BEI) were used.



Figure 2.5. JEOL 5910LV

3. RESULTS AND DISCUSSION

3.1. Phase Analysis by XRD

XRD of S1 specimen containing mainly wollastonite, zeolite, alumina and small amount of silica and heat treated at 1000°C indicates mainly wollastonite and alumina phases (Fig.3.1). A small amount of anorthite phase also formed at this temperature indicating that anorthite formation started at 1000°C. As the temperature increased, the amount of anorthite phase also increased. But the major phases were still wollastonite and alumina at 1100°C. As the temperature was increased to 1200°C, the anorthite phases increased significantly while the content of wollastonite and alumina phases decreased considerably. At 1300°C, there was mainly anorthite phase and small amount of alumina was also observed at 1300°C. This reveals that all of the wollastonite and most of the alumina phases were converted to anorthite phase.

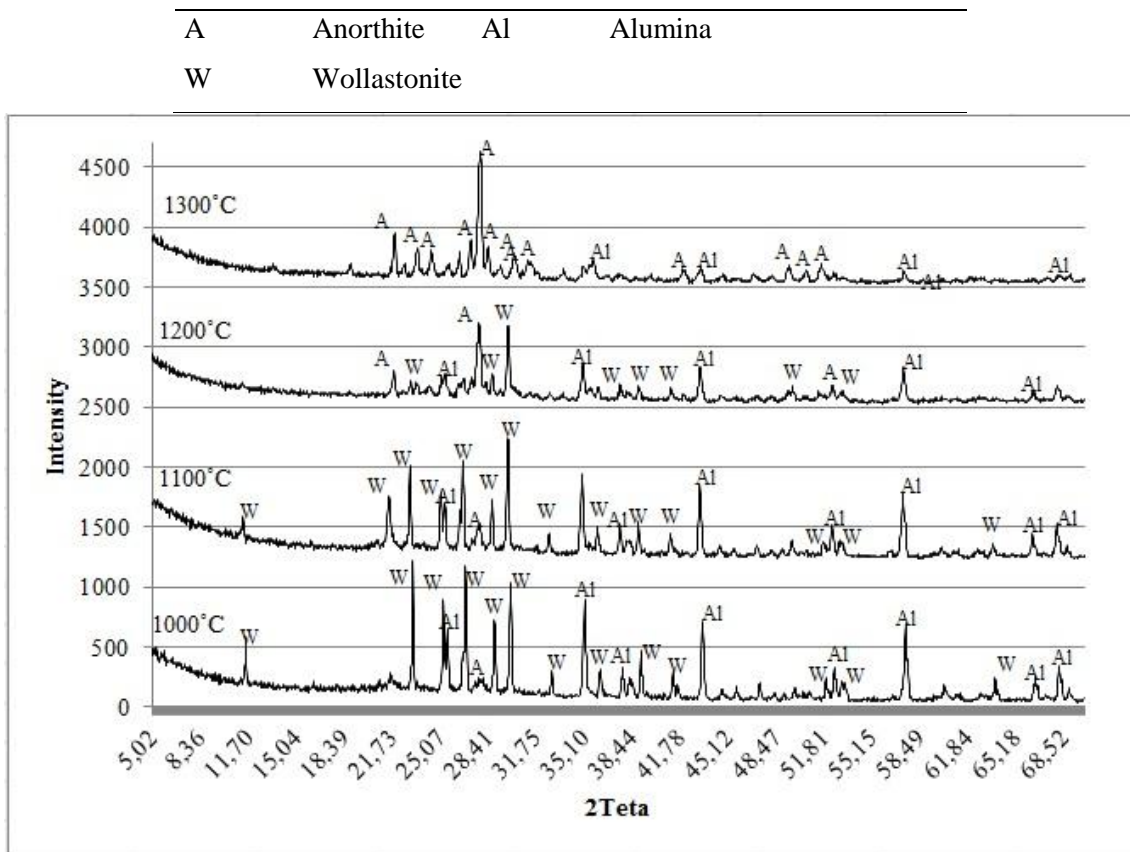


Figure 3.1. XRD pattern of S1 specimen at different temperatures

XRD of S2 specimen sintered at 1000°C indicates mainly wollastonite and alumina phases since this specimen includes starting materials of wollastonite, kaolinite and alumina (Fig.3.2). In addition, small amount of anorthite phase was also observed at this temperature. As temperature increased to 1100°C, the phases did not change comparing to 1000°C. The intensity of anorthite peaks was nearly similar with 1000°C. But increasing temperature to 1200°C increased the amount of anorthite phase while the amounts of wollastonite and alumina phases decreased considerably. Nevertheless, no other phases formed at this temperature. Increasing the heat treatment temperature to 1300°C gave only single phase anorthite showing that all the wollastonite and alumina reacted to form anorthite.

A	Anorthite	Al	Alumina
W	Wollastonite		

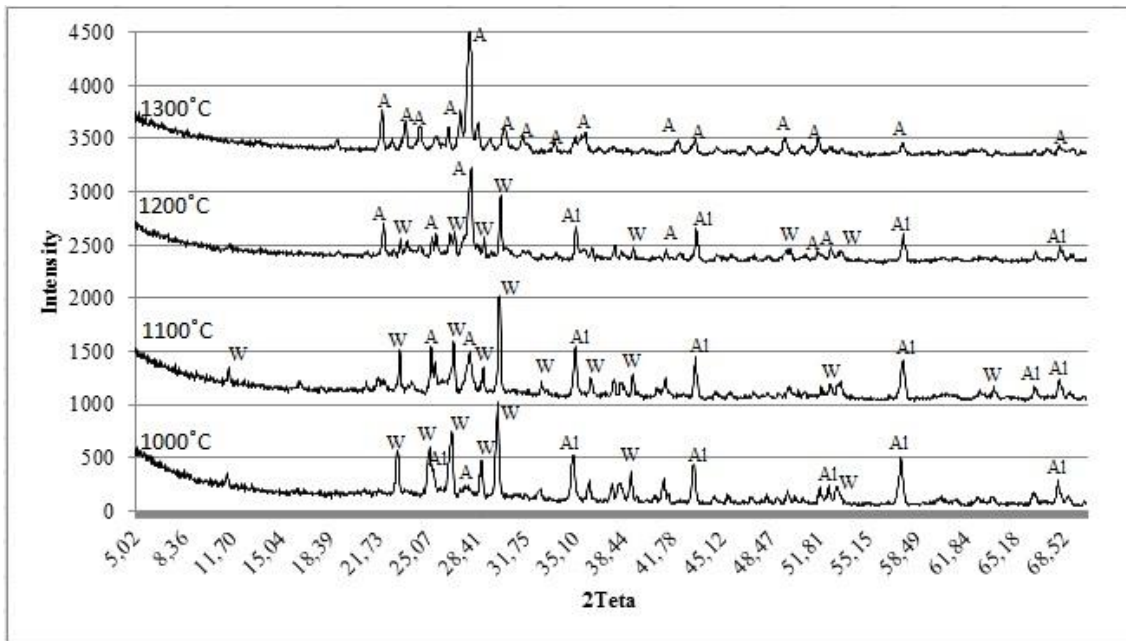


Figure 3.2. XRD pattern of S2 specimen at different temperatures

XRD of S3 specimen indicates that gehlenite, anorthite and alumina phases occurred at 1000°C (Fig.3.3). S3 specimen contains zeolite, kaolinite, alumina and calcium carbonate as starting materials. Formation of gehlenite phase was due to existence of calcium oxide phase. As temperature was increased to 1100°C, the gehlenite and anorthite phases content increased sharply but oppositely wollastonite and alumina contents decreased to low levels. Heat treatment at 1200°C led to an increase in the

content of anorthite phase but gehlenite phase content was still high at this temperature. Mainly anorthite and gehlenite phases were present at 1200°C in addition to minor amount of alumina. Increasing temperature to 1250°C, converted remaining alumina phase to gehlenite and anorthite phases resulting in two phases, gehlenite and anorthite. Increasing the temperature further to 1300°C did not cause any change in the phase content comparing to 1250°C. These results show that calcium oxide as starting material did not result in single phase anorthite formation rather gehlenite phase was coexisting together with anorthite.

A	Anorthite	Al	Alumina
G	Gehlenite		

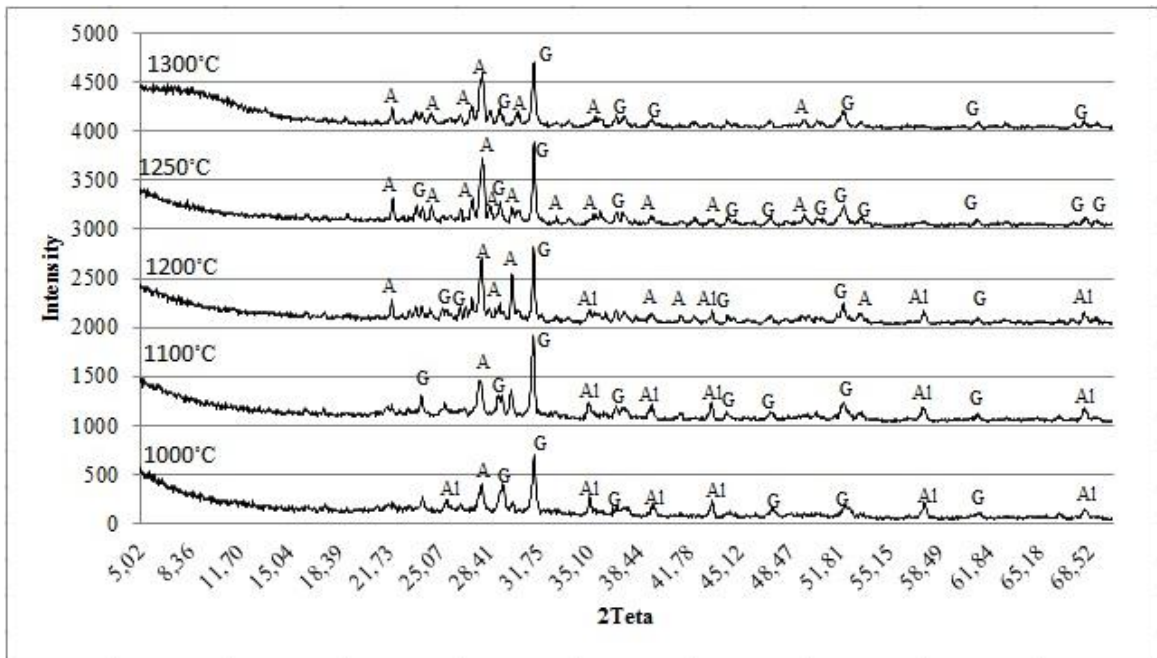


Figure 3.3. XRD pattern of S3 specimen at different temperatures

S4 specimen was same as S1 specimen that contained zeolite, wollastonite, alumina and quartz. However, S4 specimen had 1% of boron oxide (B_2O_3) as flux. XRD of S4 specimen indicated that there were wollastonite, alumina and quartz phases at 1000°C (Fig.3.4). In addition, a small amount of anorthite phase was also detected at this temperature. But in S1 specimen no quartz phase was observed. This revealed that boron oxide accelerated the formation of anorthite phase. Moreover, there was also unreacted SiO_2 that did not convert to anorthite. As temperature was raised to 1100°C, anorthite phase increased but there were still high amount of wollastonite, alumina and

quartz phases. But no quartz phase was detected in the XRD of S1 specimen at 1100°C. As the temperature was increased to 1200°C, the anorthite phase increased considerably, but oppositely the content of wollastonite and alumina phases decreased. The XRD of S1 and S4 heat treated at 1200°C were identical. Increasing temperature to 1250°C led to formation of nearly single phase except for small amount of alumina. Rising the heat treatment temperature to 1300°C gave single phase anorthite phase. No any other second phases were observed. However, S1 specimen at the same temperature (1300°C) did not result in single anorthite phase formation that also a small amount of alumina was detected. This clearly indicates that boron oxide accelerate the formation of anorthite.

A	Anorthite	Al	Alumina
W	Wollastonite	Q	Quartz

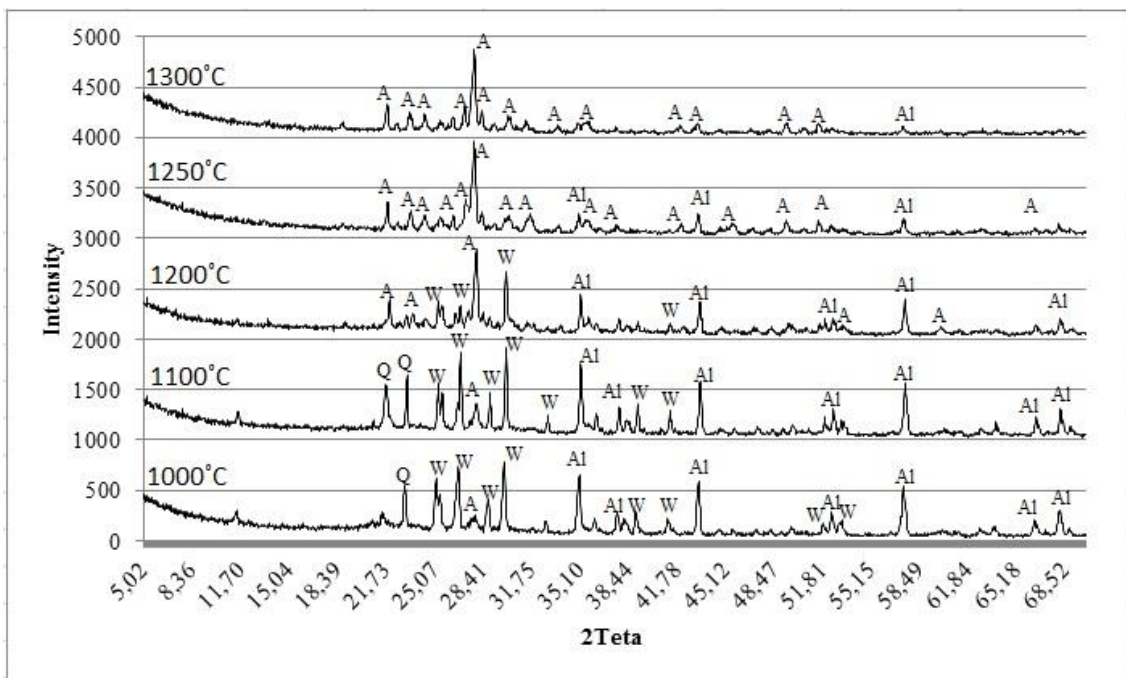


Figure 3.4. XRD pattern of S4 specimen at different temperatures

XRD of S1, S2, S3 and S4 specimens heat treated at 1000°C indicated that the raw materials were still present at this temperature (Fig.3.5). There were mainly wollastonite and alumina phases. But a significant amount of gehlenite phase was observed in S3 specimen. This was due to CaO starting material in S3. A small amount of anorthite phase formed at all of the samples. These results show that employment of CaO as starting material led to formation of gehlenite phase. The difference between S1 and S4

at 1000°C was due to addition of boron oxide into the S4, although the other starting materials were totally identical in S1 and S4. Addition of boron oxide led to formation of lower amount of wollastonite and alumina phases and additional quartz phase.

A	Anorthite	Al	Alumina
W	Wollastonite	G	Gehlenite

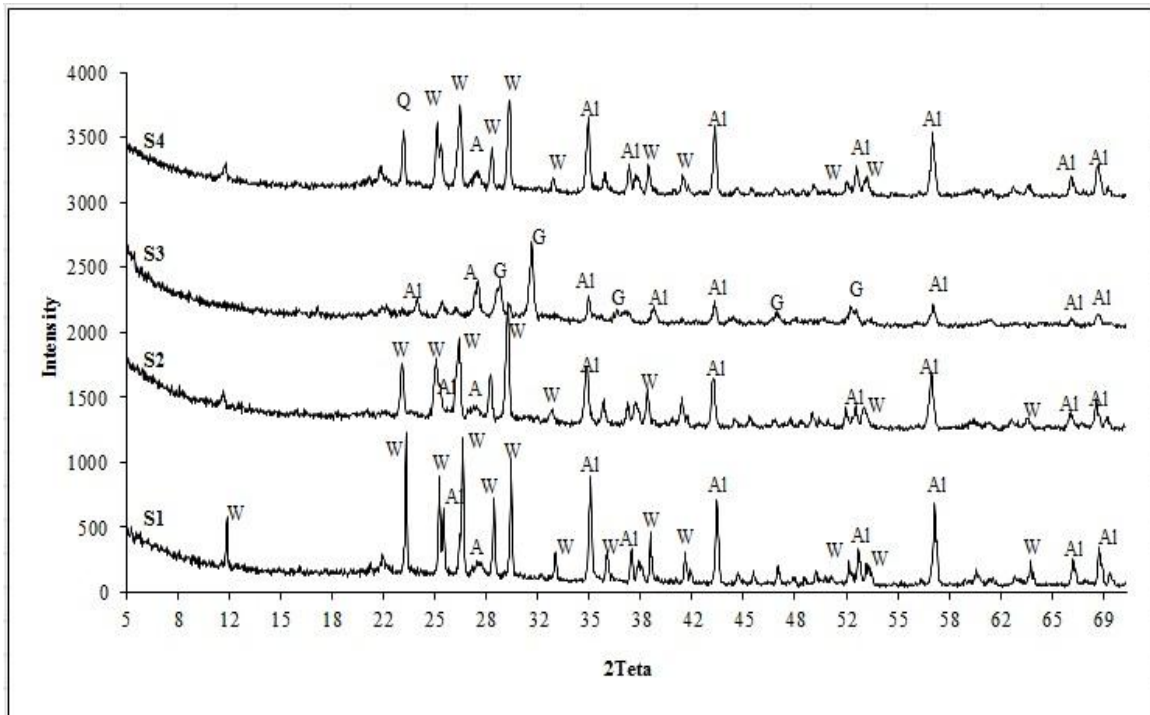


Figure 3.5. XRD pattern of all four specimens at 1000°C

XRD of S1, S2, S3 and S4 specimens' heat treated at 1100°C indicated that no single phase anorthite was obtained (Fig.3.6). Although the same starting raw materials were used in S1 and S4, high amount of quartz phase formed in S4 due to boron oxide addition but not formed in S4. The gehlenite phase only formed in S3 where CaO was used as starting material. The intensity of the peaks that were belong to the anorthite was identical in all four samples (S1, S2, S3 and S4).

A	Anorthite	Al	Alumina
W	Wollastonite	G	Gehlenite

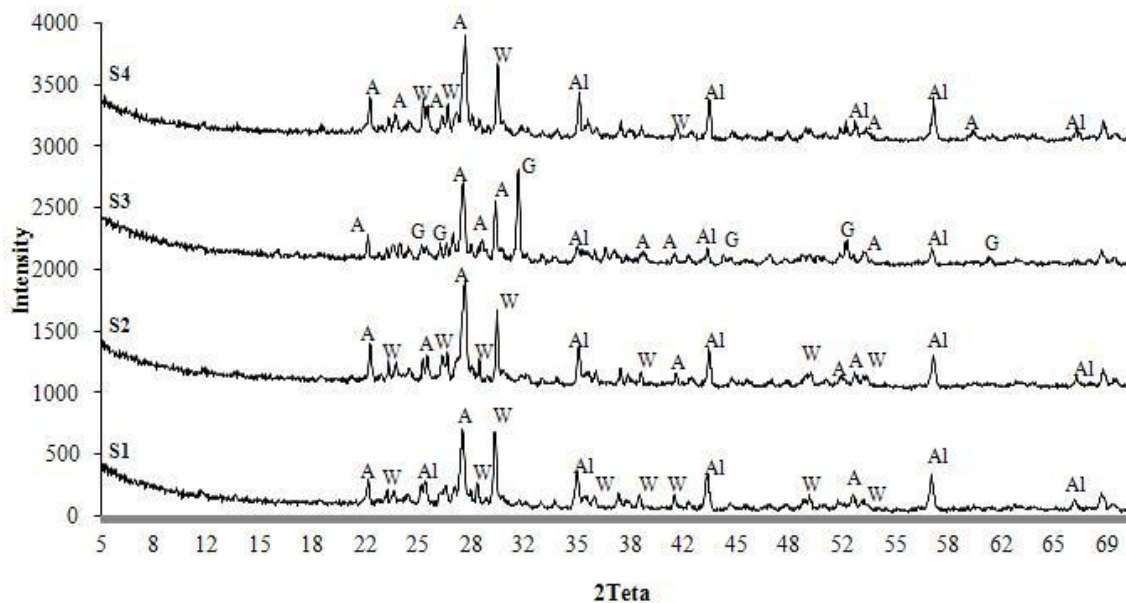


Figure 3.7. XRD pattern of all four specimens at 1200°C

XRD of S1, S2, S3 and S4 heat treated at 1300°C indicated that single phase anorthite was obtained in S2 and S4 (Fig.3.8). But although mostly anorthite phase formed in S1, a small amount of alumina phase was detected together with anorthite. Although S1 and S4 samples included same starting materials, formation of single anorthite phase in S4 at 1300°C (but not in S1) can be explained due to addition of boron oxide into S4 which accelerated the formation of anorthite. Nevertheless, S3 sample indicated two major phases at 1300°C that were anorthite and gehlenite. This could be explained due to CaO used as starting material in S3. It shows that formation of gehlenite doesn't result in anorthite formation probably due to slow transformation of gehlenite to anorthite. Because in S3 high amount of gehlenite formed even at 1000°C which could not be converted into anorthite due to slow reaction rate.

A	Anorthite	Al	Alumina
G	Gehlenite		

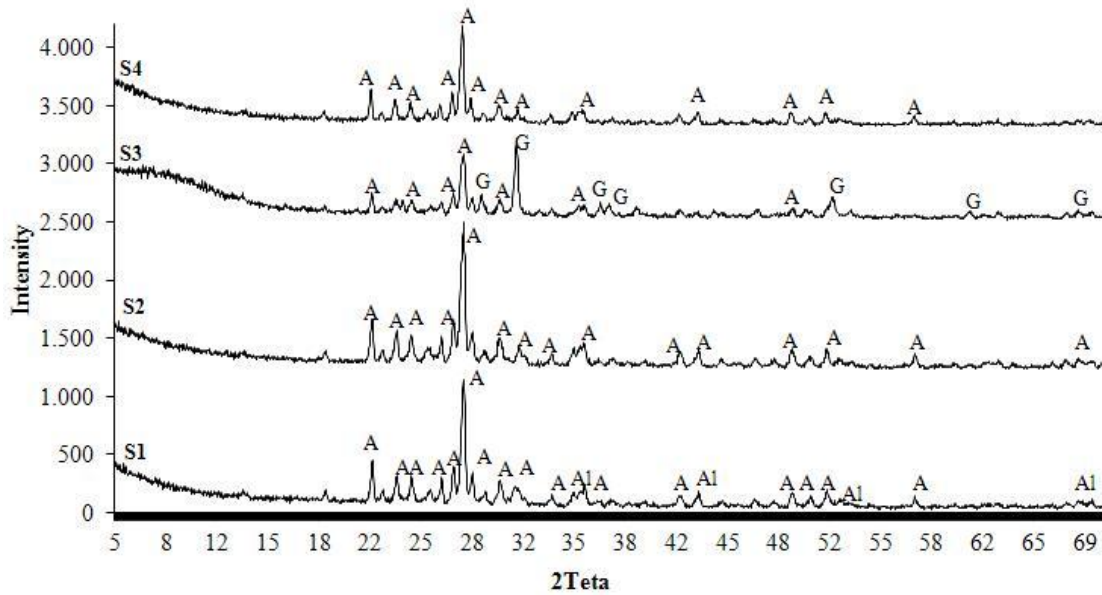


Figure 3.8. XRD pattern of all four specimens at 1300°C

Usage of CaO as starting material in addition to zeolite, kaolinite and alumina (S3) gave mainly gehlenite phase ($\text{Ca}_2\text{Al}_2\text{SiO}_7$ or $2\text{CaO} \cdot \text{Al}_2\text{O}_3 \cdot \text{SiO}_2$) and did not result in single anorthite phase formation. It can be said that conversion of gehlenite to anorthite was very slow since gehlenite phase in S3 formed even at 1000°C and did not transform to anorthite at higher temperatures of 1300°C. So this led to formation of gehlenite anorthite phases together in S3 even at high temperature of 1300°C. But starting with S1 (wollastonite, zeolite, alumina) and S2 (wollastonite, kaolinite, alumina) gave single phase anorthite, although a small fraction of alumina existed at 1300°C in case of S1. Addition of boron oxide had positive effect on anorthite formation i.e. it accelerated the formation of anorthite.

3.2. Densities of Anorthite Ceramics

The relative densities of the samples are given for each sintering temperature in Table 3.1. Also, it is important to highlight that the theoretical densities of the samples should be calculated considering the weight fractions of each phase at each specific sintering temperature. Because the theoretical density of the sample may change depends on the present phases and their weight fraction at a specific sintering temperature.

Table 3.1.Relative densities of the samples at different temperatures

	d(mm)	h(mm)	W _a	W _b	W _c	V (cm ³)	D=W _a /V	D _{apparent} W _a /(W _a - W _b)	Relative Density %*	
1000 °C	S1	10,500	1,300	0,141	0,094	0,191	0,113	1,255	2,968	89,68
	S2	10,540	1,540	0,187	0,121	0,227	0,134	1,389	2,855	92,39
	S3	10,300	1,530	0,169	0,109	0,217	0,127	1,325	2,819	90,94
	S4	10,550	2,700	0,230	0,149	0,299	0,236	0,973	2,831	89,59
1100 °C	S1	10,600	2,700	0,223	0,146	0,290	0,238	0,935	2,886	88,26
	S2	10,000	1,100	0,137	0,091	0,180	0,086	1,582	2,965	93,84
	S3	10,800	1,100	0,094	0,061	0,132	0,101	0,935	2,795	91,35
	S4	10,500	1,600	0,206	0,134	0,265	0,139	1,485	2,854	90,33
1200 °C	S1	10,500	1,600	0,209	0,129	0,259	0,139	1,508	2,624	85,48
	S2	10,600	1,300	0,196	0,123	0,237	0,115	1,706	2,703	88,62
	S3	10,300	1,200	0,130	0,081	0,177	0,100	1,296	2,683	88,85
	S4	10,500	1,700	0,228	0,138	0,286	0,147	1,547	2,533	82,05
1250 °C	S3	8,520	1,080	0,125	0,079	0,062	2,022	74,228	2,730	93,82
	S4	9,270	1,160	0,144	0,089	0,078	1,842	67,616	2,612	80,88
1300 °C	S1	9,210	1,620	0,163	0,103	0,108	1,512	55,512	2,706	92,37
	S2	9,600	1,610	0,170	0,107	0,117	1,460	53,616	2,697	97,73
	S3	8,310	1,180	0,109	0,067	0,064	1,695	62,237	2,589	89,29
	S4	8,730	1,380	0,146	0,091	0,083	1,763	64,708	2,667	96,62

*: The relative densities were calculated using the theoretical density values given in Table 3.2 which were calculated according to the weight fraction of phases.

Table 3.2. Theoretical densities of samples and raw material distribution at different temperatures

S 1							Theoretical density
%		Wollastonite	Alumina	Anorthite	Gehlenite	Silica	(g/cm ³)
1000°C	51,89	37,9	10,12	0	0	3,31	
1100°C	49,05	35,38	15,56	0	0	3,27	
1200°C	38,85	20,57	40,57	0	0	3,07	
1300°C	0	13,63	86,36	0	0	2,93	

S 2							Theoretical density
%		Wollastonite	Alumina	Anorthite	Gehlenite	Silica	(g/cm ³)
1000°C	50,36	20,14	29,49	0	0	3,09	
1100°C	49,27	26,09	24,64	0	0	3,16	
1200°C	34,01	19,28	46,7	0	0	3,05	
1300°C	0	0	100	0	0	2,76	

S 3							Theoretical density
%		Wollastonite	Alumina	Anorthite	Gehlenite	Silica	(g/cm ³)
1000°C	37,03	18,96	26,83	17,17	0	3,10	
1100°C	49,27	26,09	24,64	0	0	3,16	
1200°C	0	10,59	41,47	47,94	0	3,02	
1300°C	0	0	49,04	50,95	0	2,90	

S 4							Theoretical density
%		Wollastonite	Alumina	Anorthite	Gehlenite	Silica	(g/cm ³)
1000°C	30,27	25,29	28,35	16,08	0	3,16	
1100°C	38,93	33,11	0	0	27,96	3,16	
1200°C	32,83	22,39	44,78	0	0	3,09	
1300°C	0	0	100	0	0	2,76	

According to theoretical density values (Table 3.2.), a density variation graph was accomplished. Except 1200°C, the density continued to rise regularly. But, at 1200°C, a

sharp decrease was observed for all of the samples. It is also pointed out what caused that decrement on the density at 1200°C. And that negative change on density at 1200°C can be studied as futurework.

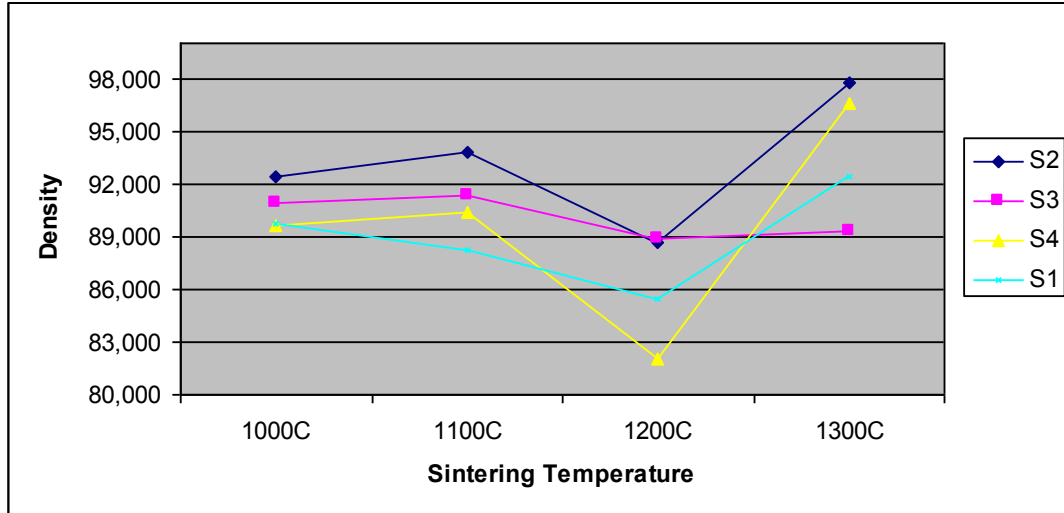


Figure.3.9. The density variation of the samples sintered at different temperatures

3.3. Microstructure Analysis Examined by SEM-EDS

Scanning Electron Microscopy of S1 specimen containing mainly wollastonite, zeolite, alumina and small amount of silica and heat treated at 1250°C and 1350°C indicated only anorthite phase (Fig. 3.10 and 3.11) as observed in XRD which revealed single anorthite phase at 1300°C (Fig.3.8). EDS analysis taken from different regions gave a composition which is very near to the theoretical composition values of anorthite phase (Fig. 3.12).

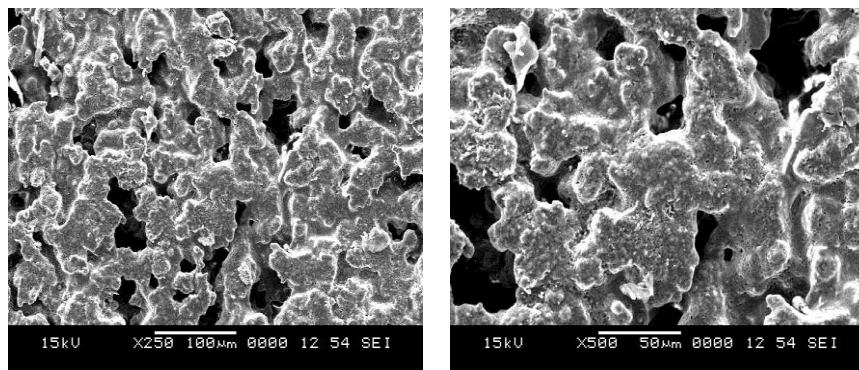


Figure 3.10. Secondary electron image of S1 specimen containing mainly wollastonite, zeolite, alumina and small amount of silica and heat treated at 1250°C.

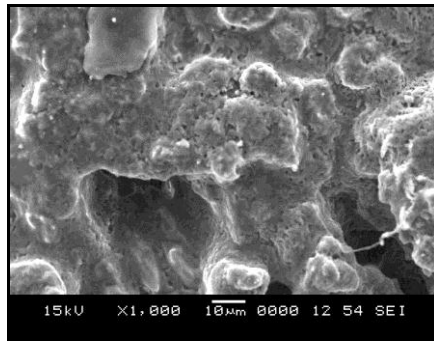


Figure 3.10. Secondary electron image of S1 specimen containing mainly wollastonite, zeolite, alumina and small amount of silica and heat treated at 1250°C(continue).

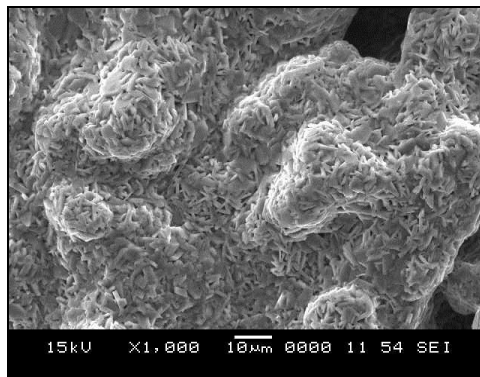
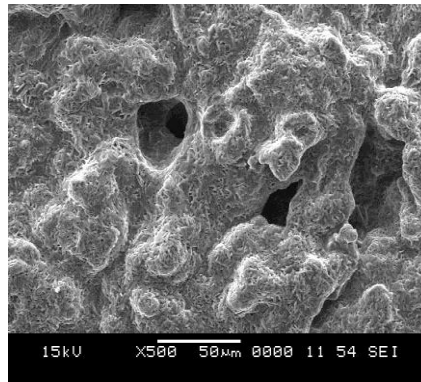
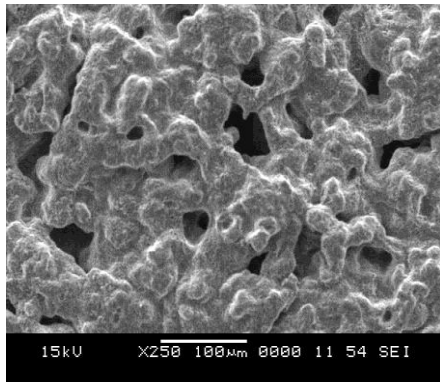


Figure 3.11. Secondary electron image of S1 specimen containing mainly wollastonite, zeolite, alumina and small amount of silica and heat treated at 1350°C.

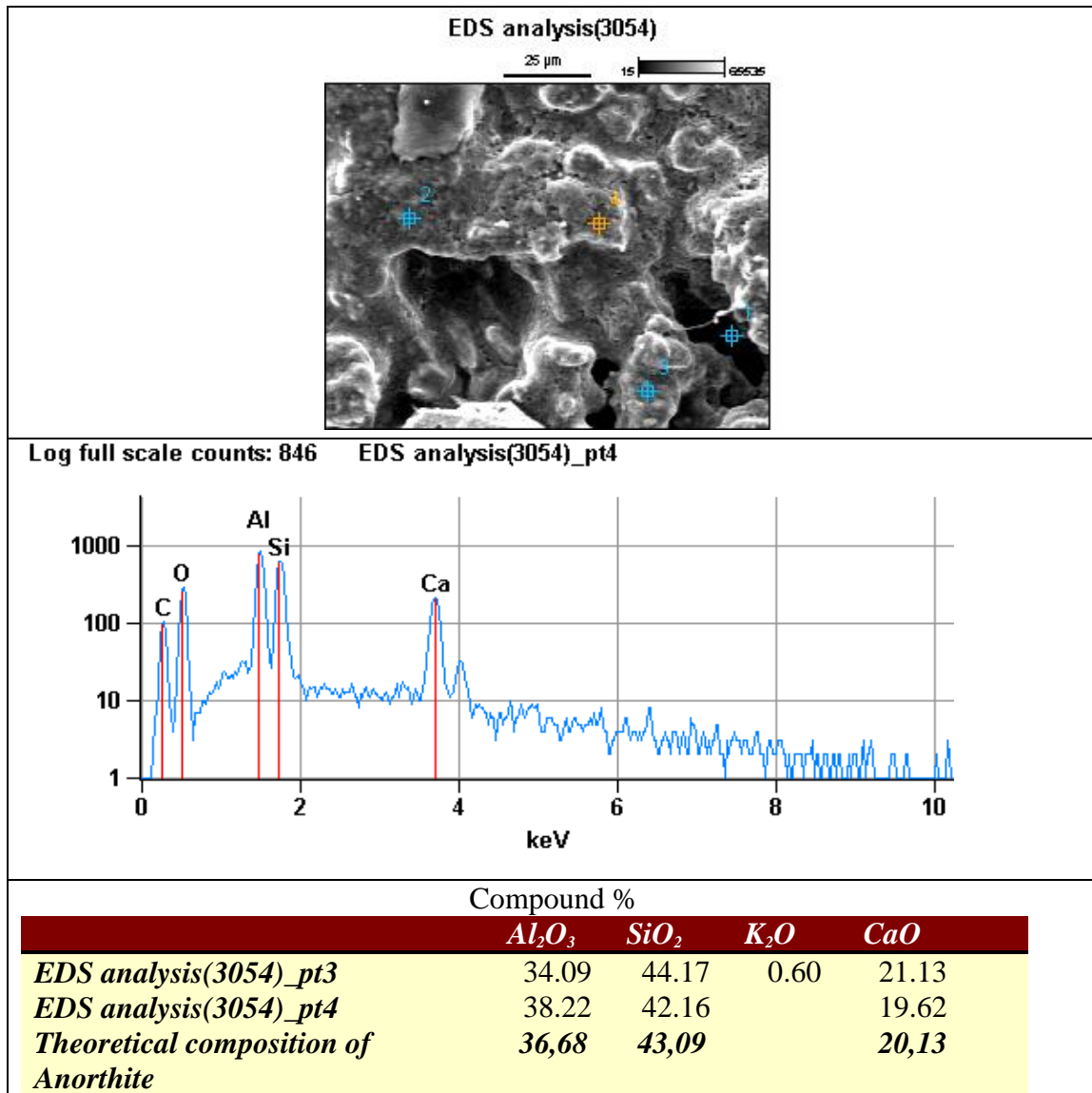


Figure 3.12. EDS analysis of S1 specimen heat treated at 1250°C (S1 contains mainly wollastonite, zeolite, alumina and small amount of silica). a) SEM micrograph showing EDS points, b) EDS analysis from anorthite phase, c) Chemical analysis of phases determined in EDS.

SEM of S2 specimen sintered at 1150°C indicates mainly wollastonite and alumina phases (Fig.3.13). XRD analysis also reveals wollastonite and alumina phases (Fig.3.2). However, SEM revealed mostly anorthite phase at 1250°C in addition to small amount of wollastonite phase. EDS analysis taken from different grains indicated that the longitudinal grains were belong to the wollastonite phase (Fig.3.14). The rounded grains were anorthite phase.

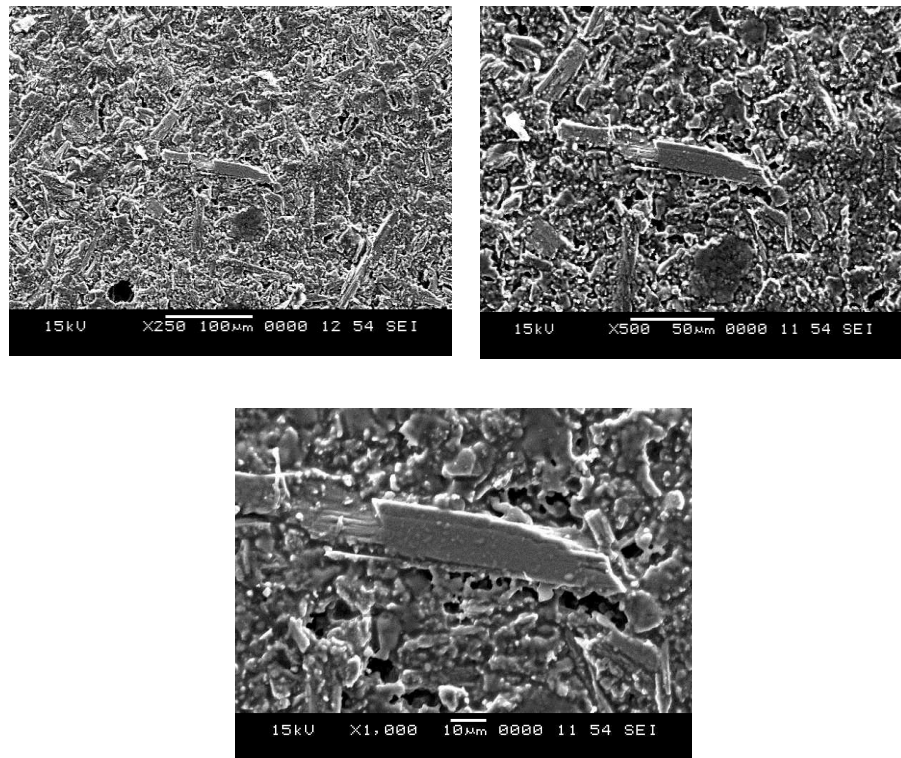


Figure 3.13. Secondary electron image of S2 specimen containing mainly wollastonite, zeolite, alumina and small amount of silica and heat treated at 1150°C.

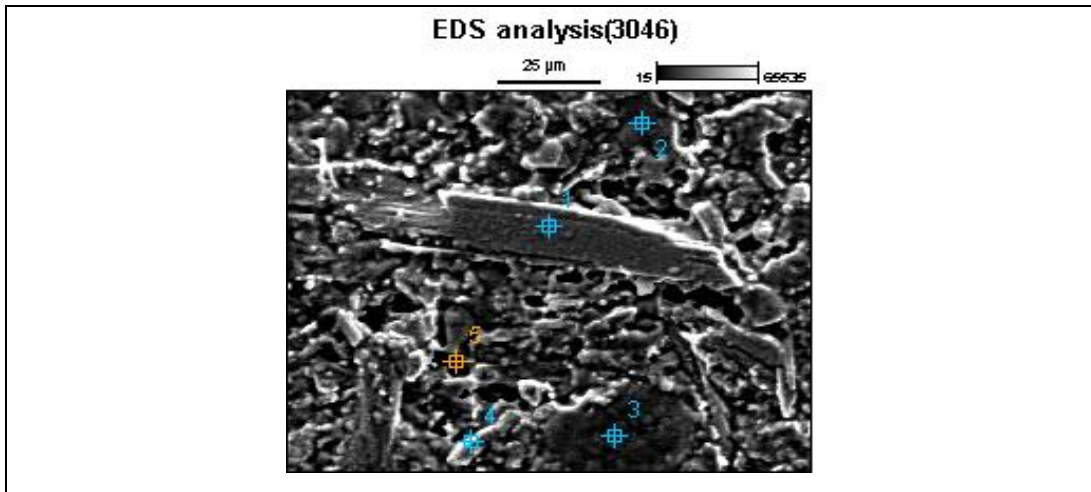


Figure 3.14. EDS analysis of S2 specimen heat treated at 1150°C (S2 contains mainly wollastonite, zeolite, alumina and small amount of silica). a) SEM micrograph showing EDS points, b) EDS analysis from anorthite phase, c) EDS analysis from wollastonite phase and d) Chemical analysis of phases determined in EDS

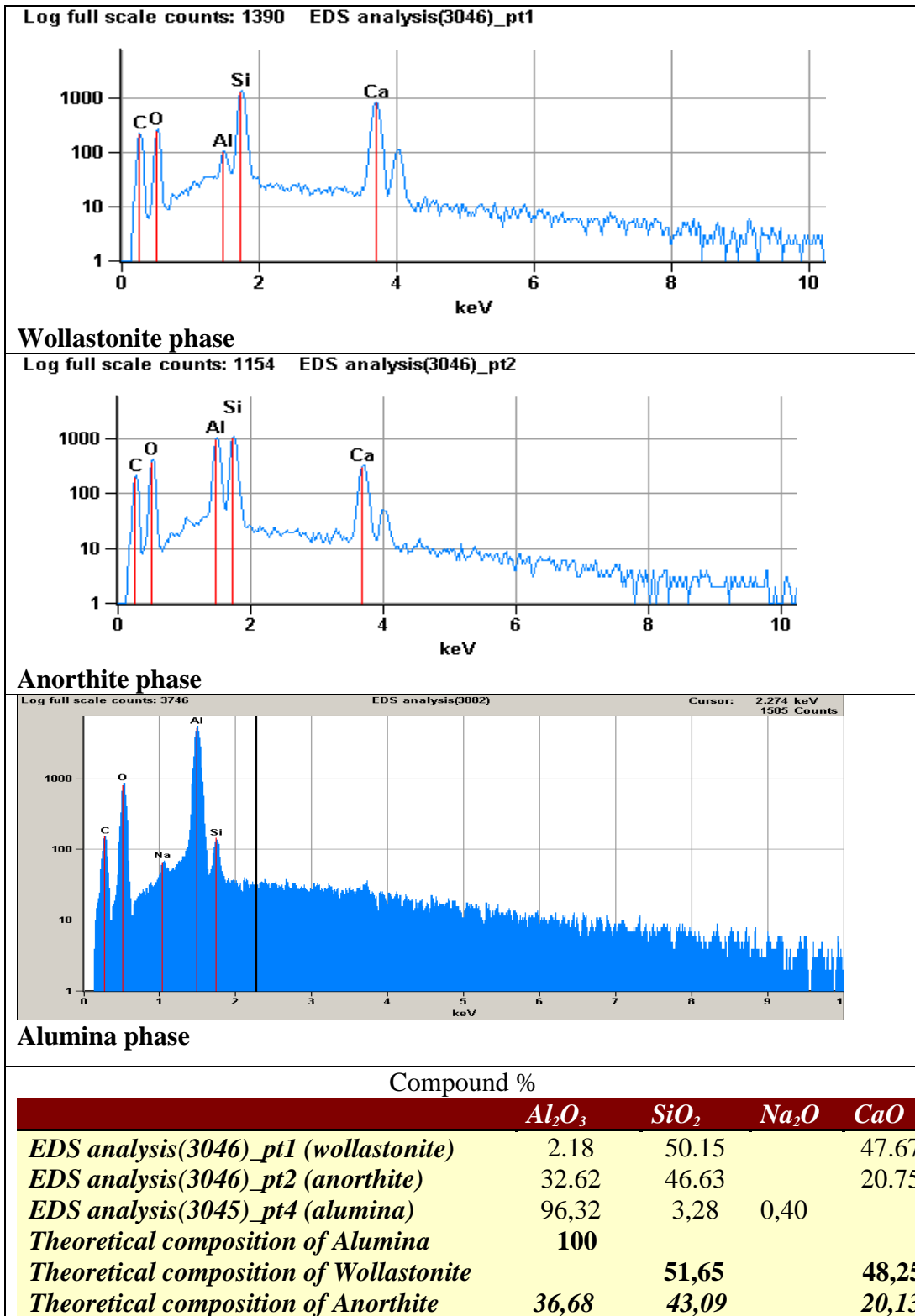


Figure 3.14. EDS analysis of S2 specimen heat treated at 1150°C (S2 contains mainly wollastonite, zeolite, alumina and small amount of silica). a) SEM micrograph showing EDS points, b) EDS analysis from anorthite phase, c) EDS analysis from wollastonite phase and d) Chemical analysis of phases determined in EDS (continue).

SEM of S3 specimen sintered at 1100°C for 1 h indicated wollastonite, gehlenite, alumina and anorthite phases (Fig. 3.15). EDS analysis of the phases were near to the theoretical composition values (Fig. 3.16).

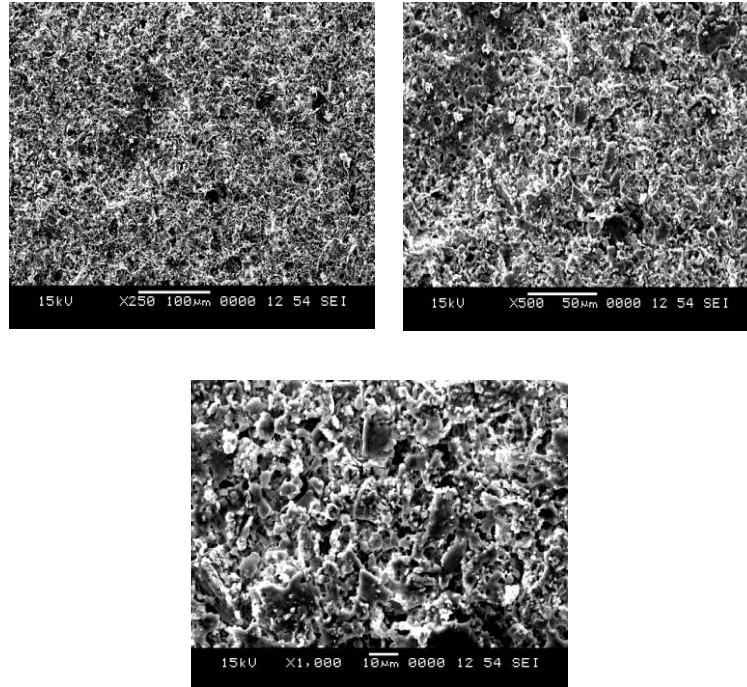


Figure 3.15. Secondary electron image of S3 specimen prepared from zeolite, kaolinite, calcium carbonate and heat treated at 1100°C.

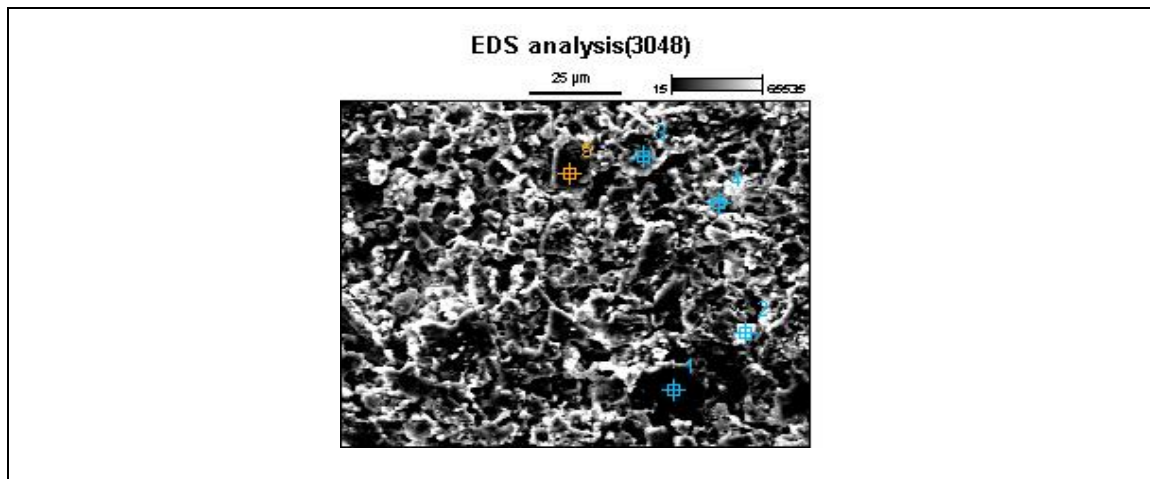


Figure 3.16. EDS analysis of S3 specimen heat treated at 1100°C (S3 contains zeolite, kaolinite, alumina and calcium carbonate).a) SEM micrograph showing EDS points,b) EDS analysis from anorthite phase,c)EDS analysis from alumina phase, d) EDS analysis from wollastonite phase, e) EDS analysis from gehlenite phase and f) Chemical analysis of phases determined in EDS

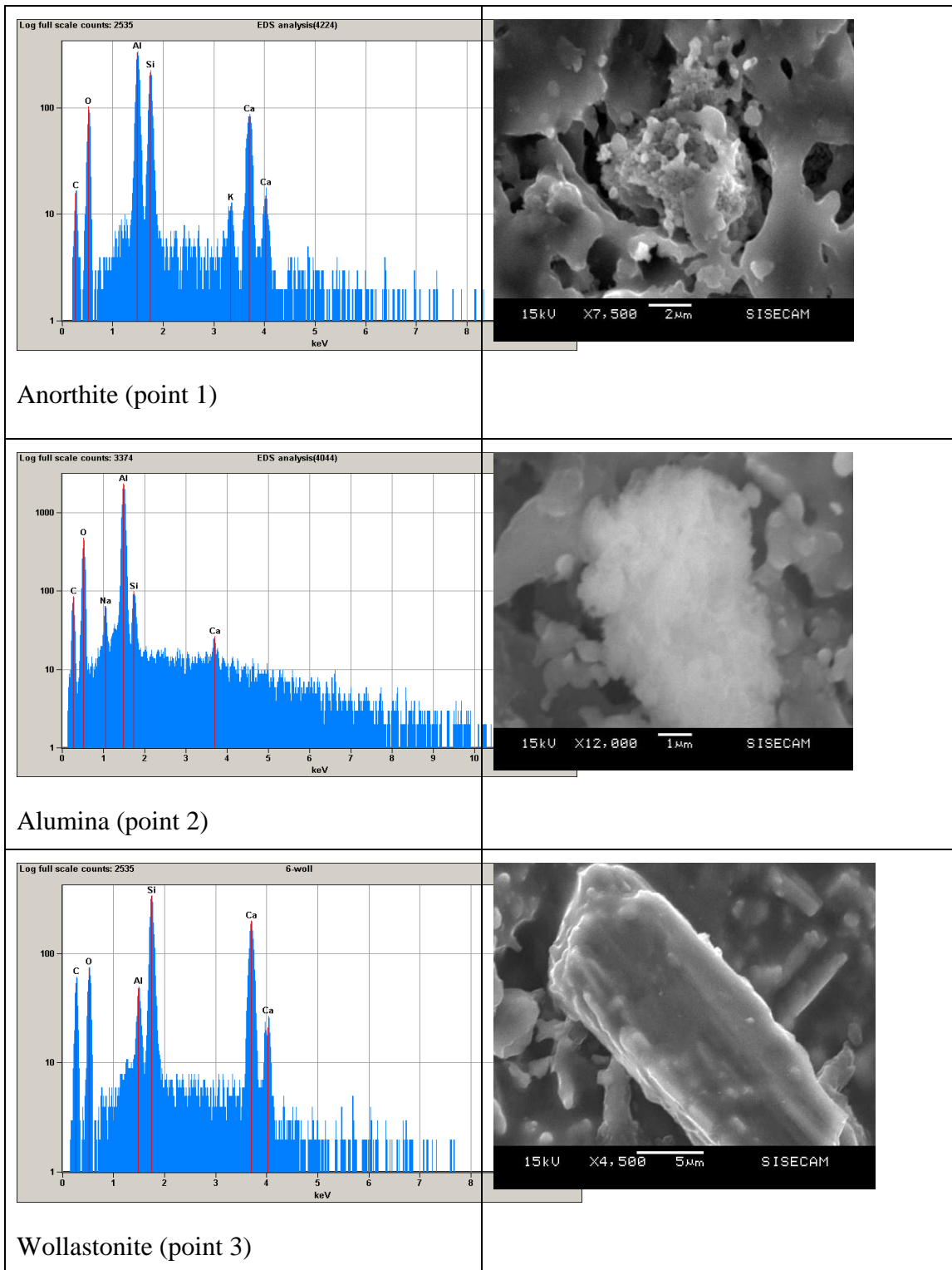


Figure 3.16. EDS analysis of S3 specimen heat treated at 1100°C (S3 contains zeolite, kaolinite, alumina and calcium carbonate). a) SEM micrograph showing EDS points, b) EDS analysis from anorthite phase, c) EDS analysis from alumina phase, d) EDS analysis from wollastonite phase, e) EDS analysis from gehlenite phase and f) Chemical analysis of phases determined in EDS(continue).

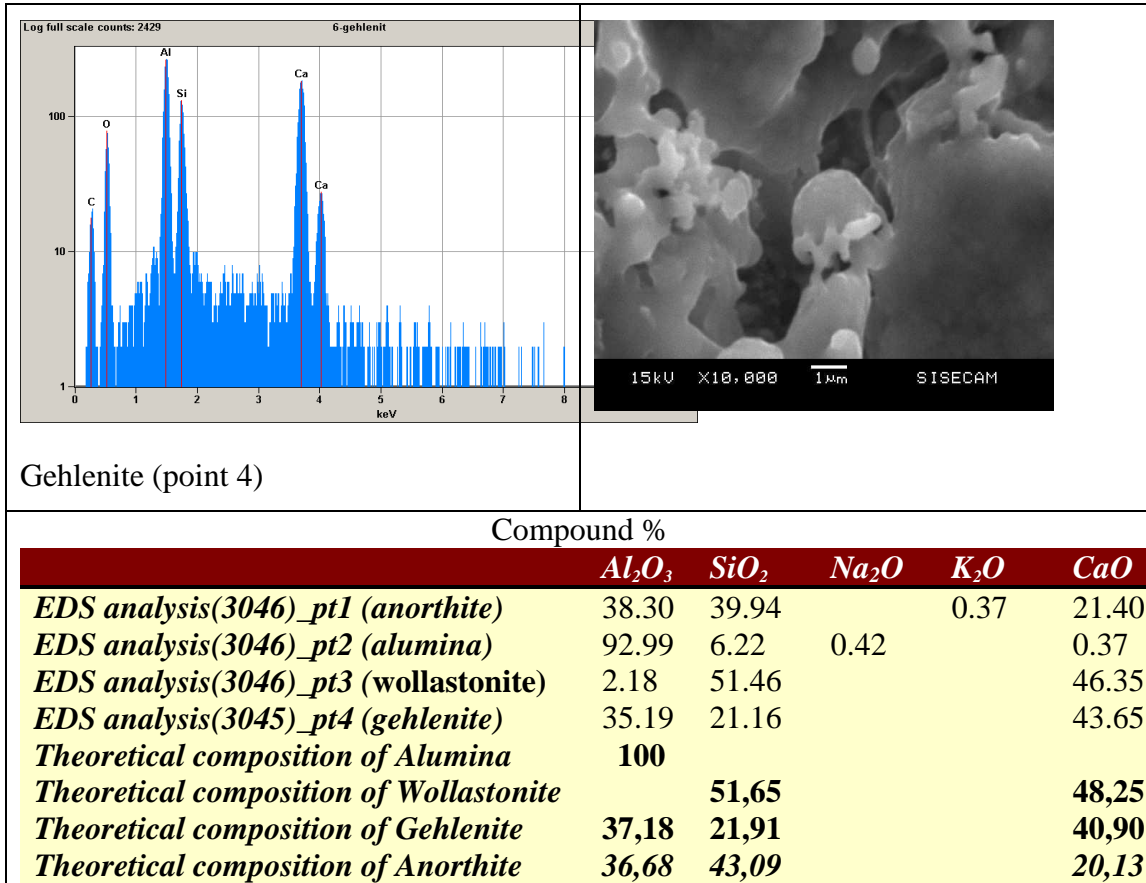


Figure 3.16. EDS analysis of S3 specimen heat treated at 1100°C (S3 contains zeolite, kaolinite, alumina and calcium carbonate). a) SEM micrograph showing EDS points, b) EDS analysis from anorthite phase, c) EDS analysis from alumina phase, d) EDS analysis from wollastonite phase, e) EDS analysis from gehlenite phase and f) Chemical analysis of phases determined in EDS(continue).

However, SEM of the S3 sample sintered at 1300°C revealed only gehlenite and anorthite phases, as observed in the XRD (Fig. 3.17). EDS analysis taken from anorthite and gehlenite phases confirmed these phases (Fig. 3.18).

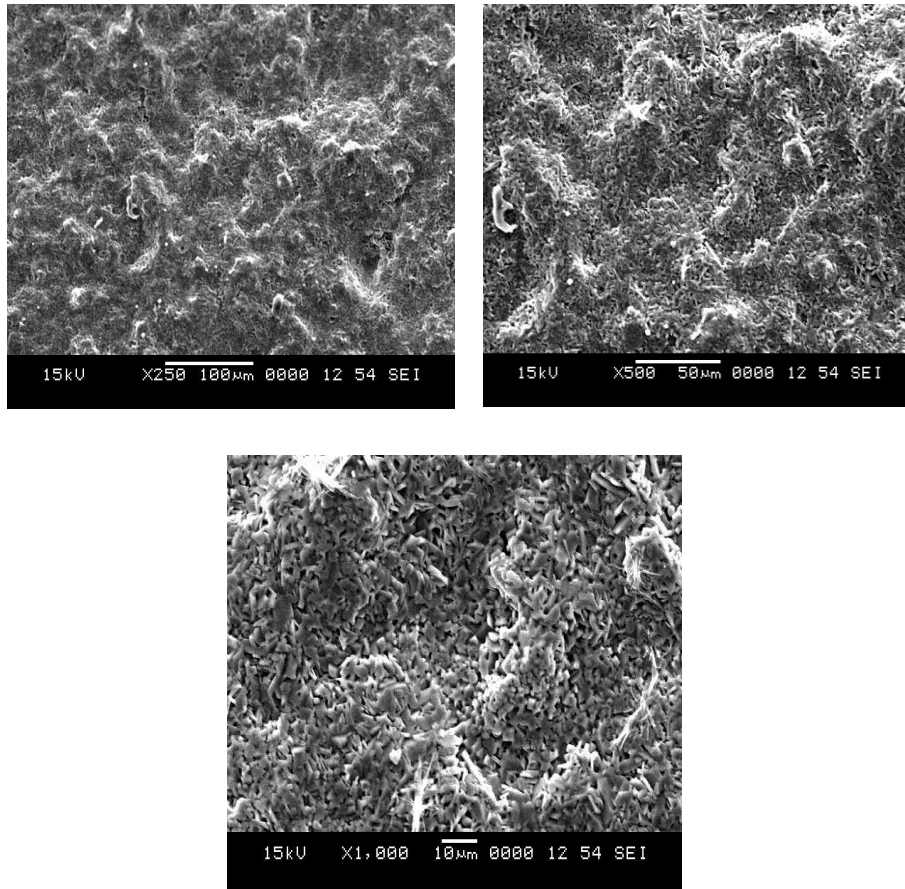


Figure 3.17. Secondary electron image of S3 specimen prepared from zeolite, kaolen, calcium carbonate and heat treated at 1300°C.

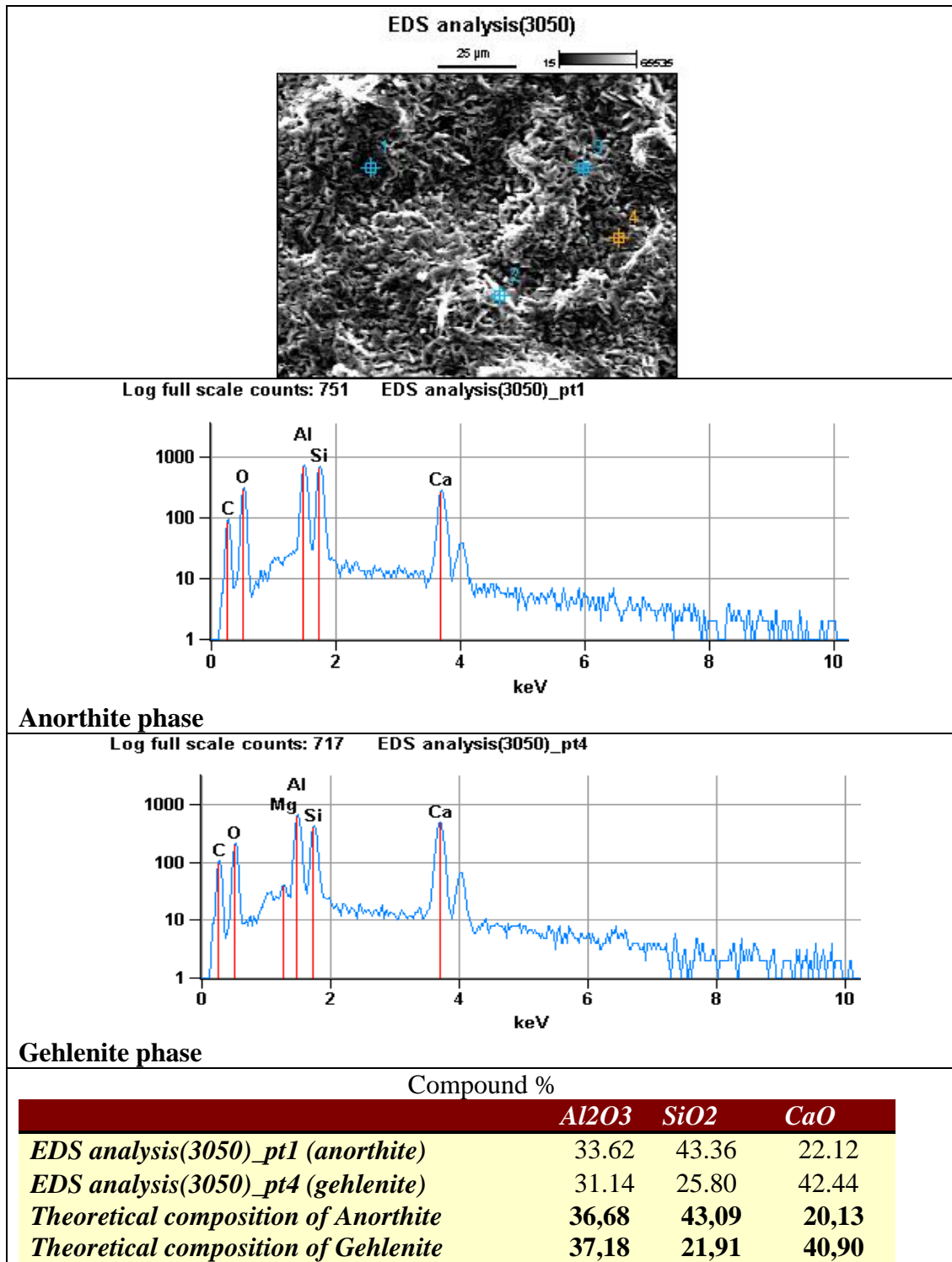


Figure 3.18. EDS analysis of S3 specimen heat treated at 1300°C (S3 contains zeolite, kaolinite, alumina and calcium carbonate). a) SEM micrograph showing EDS points, b) EDS analysis from anorthite phase, c) EDS analysis from alumina phase, d) EDS analysis from wollastonite phase, e) EDS analysis from gehlenite phase and f) Chemical analysis of phases determined in EDS.

SEM of S4 specimen sintered at 1200°C for 1 h confirmed the XRD results and showed wollastonite, anorthite and alumina phases (Fig. 3.19). EDS analysis taken from each phase was identical with theoretical composition values of appropriate phases and therefore confirmed the XRD results (Fig. 3.20).

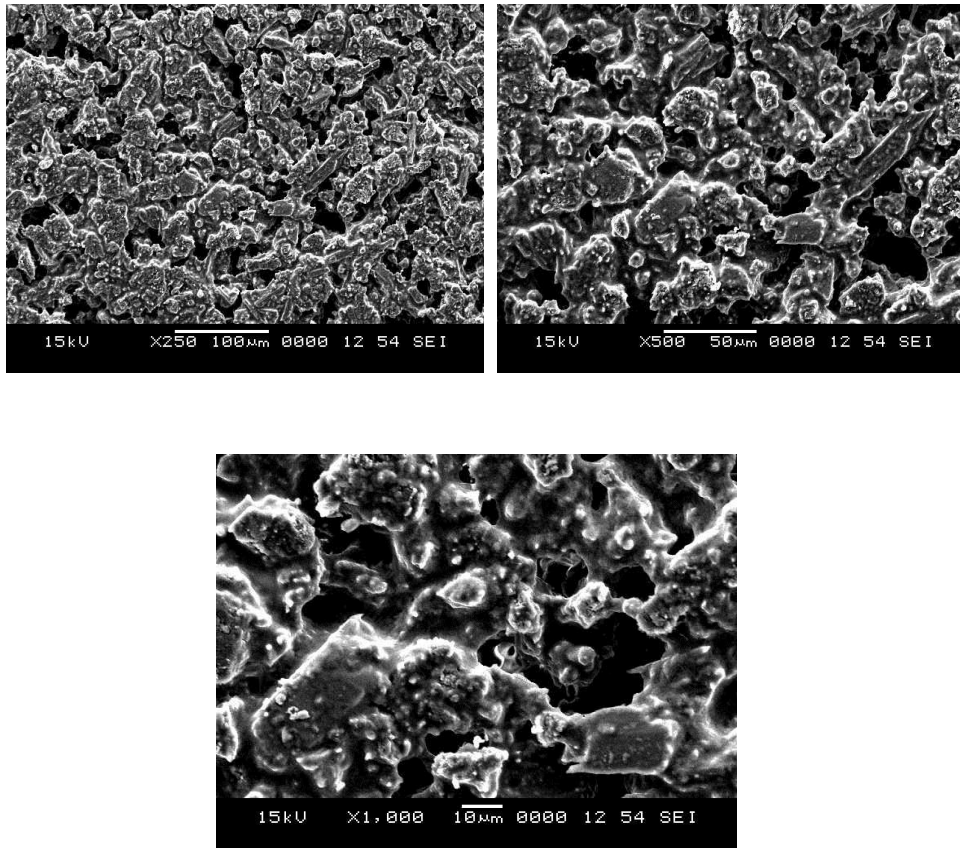


Figure 3.19. Secondary electron image of S4 specimen prepared from zeolite, wollastonite, alumina and small amount of silica and heat treated at 1200 °C.

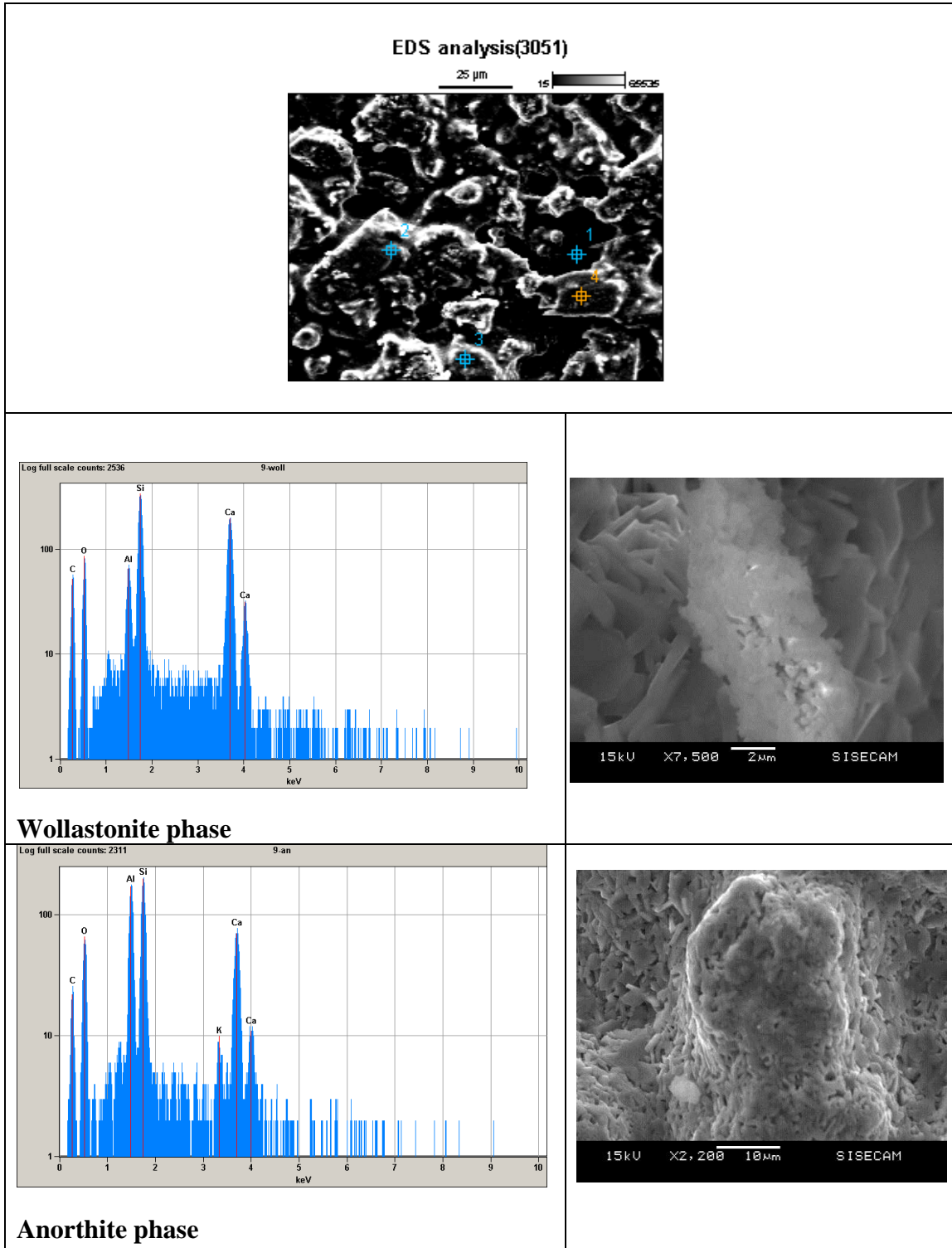
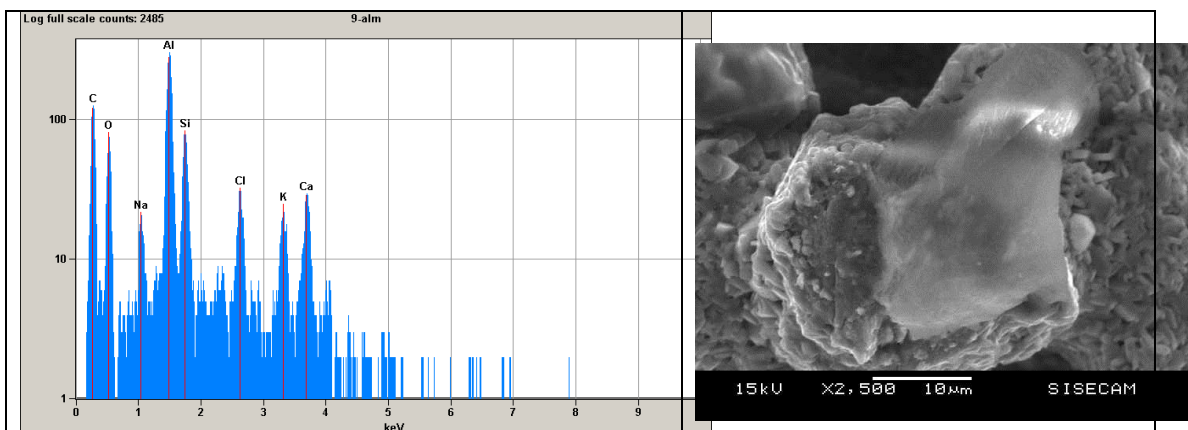


Figure 3.20. EDS analysis of S4 specimen heat treated at 1200 °C (S4 contains zeolite, wollastonite, alumina and small amount of silica). a) SEM micrograph showing EDS points, b) EDS analysis from wollastonite phase, c) EDS analysis from anorthite phase, d) EDS analysis from alumina phase and e) Chemical analysis of phases determined in EDS.



Alumina phase

	Compound %		
	<i>Al2O3</i>	<i>SiO2</i>	<i>CaO</i>
<i>EDS analysis(3050)_pt1 (wollastonite)</i>	1,31	50,28	48,41
<i>EDS analysis(3050)_pt4 (anorthite)</i>	33,68	44,39	21,43
<i>EDS analysis(3050)_pt4 (alumina)</i>	95,28	3,21	1,21
<i>Theoretical composition of Wollastonite</i>		51,65	48,25
<i>Theoretical composition of Anorthite</i>	36,68	43,09	20,13
<i>Theoretical composition of Alumina</i>	100		

Figure 3.20. EDS analysis of S4 specimen heat treated at 1200 °C (S4 contains zeolite, wollastonite, alumina and small amount of silica). a) SEM micrograph showing EDS points, b) EDS analysis from wollastonite phase, c) EDS analysis from anorthite phase, d) EDS analysis from alumina phase and e) Chemical analysis of phases determined in EDS (continue).

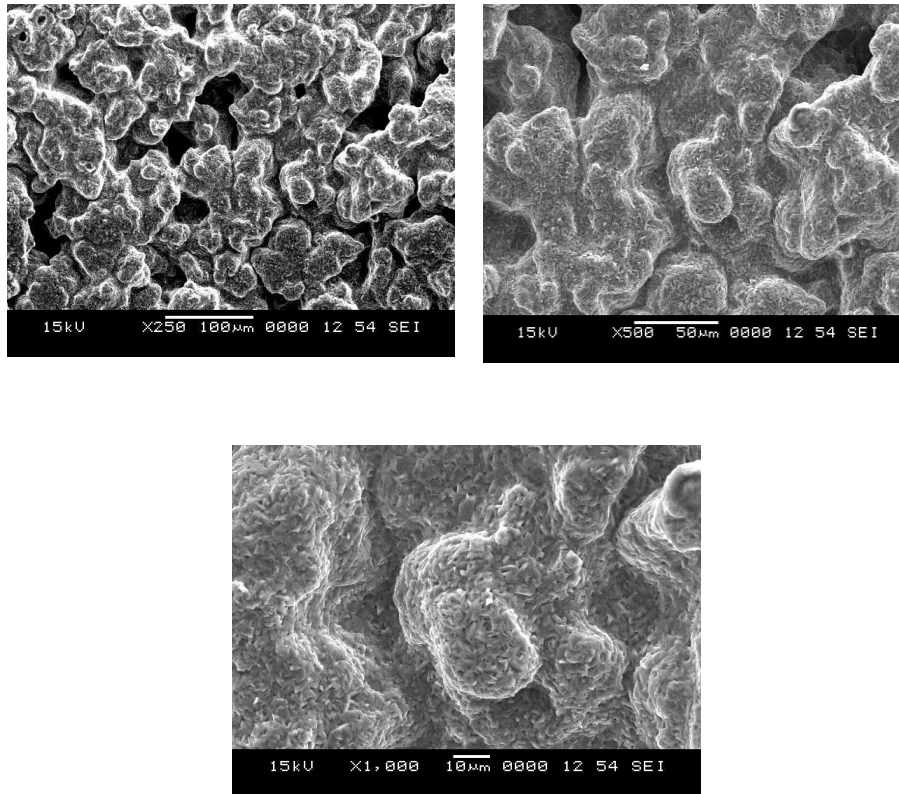


Figure 3.21. Secondary electron image of S4 specimen prepared from zeolite, wollastonite, alumina and small amount of silica and heat treated at 1350 °C.

SEM of the S4 sample sintered at 1350°C revealed only single phase anorthite (Fig. 3.21). XRD results showed that single phase anorthite formed even at 1300°C. EDS analysis from different regions confirm the single anorthite phase formation (Fig. 3.22).

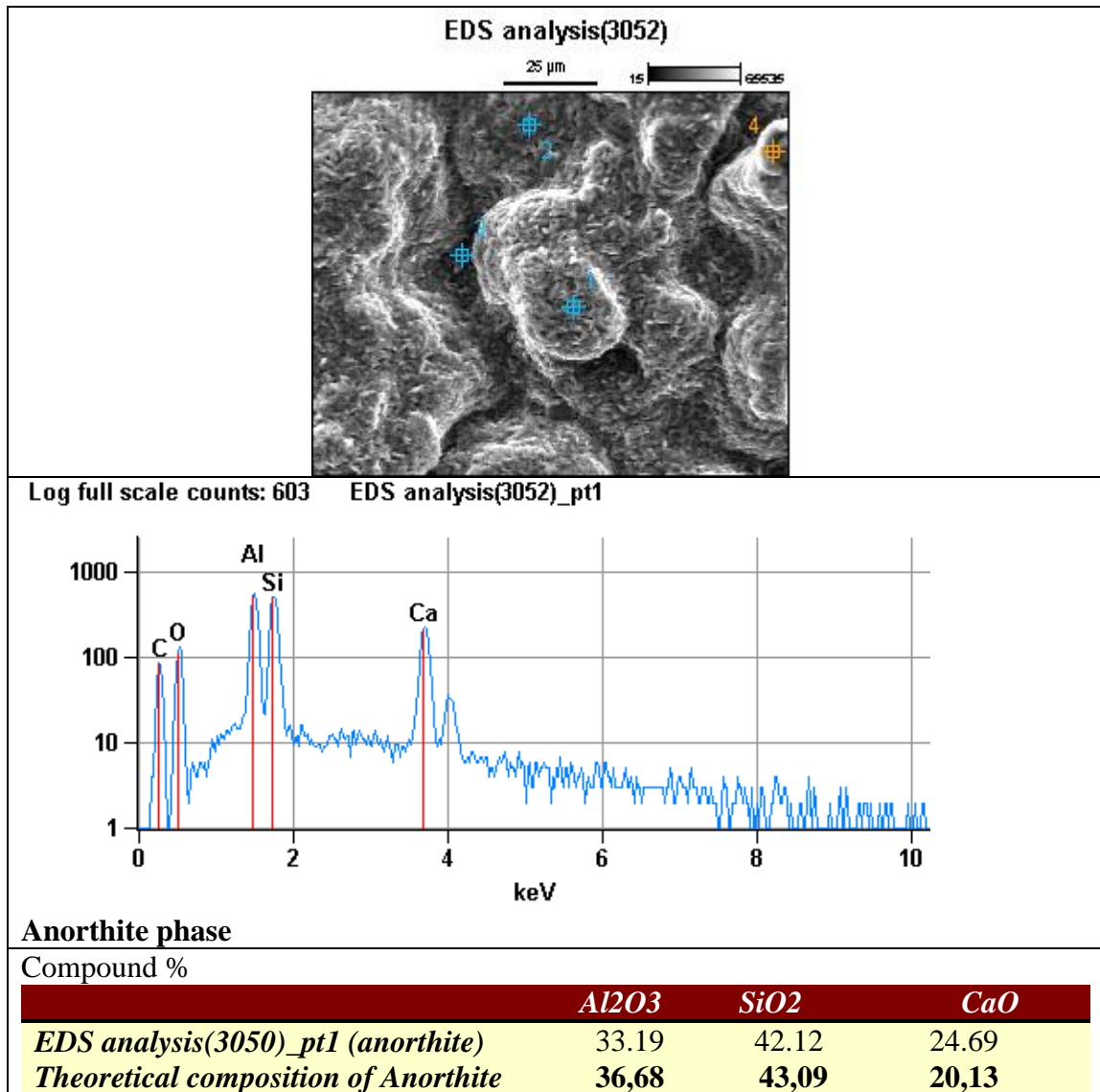


Figure 3.22. EDS analysis of S4 specimen heat treated at 1350 °C (S4 contains zeolite, wollastonite, alumina and small amount of silica). a) SEM micrograph showing EDS points, b)EDS analysis from anorthite phase and c) Chemical analysis of phases determined in EDS.

4. CONCLUSION

Local raw materials of zeolite, wollastonite, kaolinite, alumina, quartz and calcium carbonate were employed to produce anorthite ceramics since these industrial raw materials are cheap and abundant in Turkey. In one of the compositions boron oxide was also used to decrease the sintering temperature of anorthite ceramic to employ and co-fire anorthite ceramic with low melting point electrode like silver and copper which require lower sintering temperature. The main results can be summarized as follow:

1. X-ray diffraction studies indicated that starting raw materials significantly affected phase development depending on firing temperature. Starting with zeolite, wollastonite, alumina and small amount of quartz gave single phase anorthite after firing at 1300 °C for 1h. But 1 wt% boron oxide addition into the same composition accelerated the formation of anorthite.
2. Raw materials of wollastonite, kaolinite and alumina gave also single phase anorthite at 1300 °C. However, using zeolite, kaolinite, alumina and calcium carbonate did not result in single phase anorthite ceramic even at 1300 °C. CaO employment in the raw material mixture led to formation of gehlenite rather than anorthite.
3. Different raw materials had a considerable effect on densities of the anorthite ceramics at 1300 °C that lowest density was obtained when CaO was used in the starting materials possibly due to its low reactivity. Raw material composition without zeolite (wollastonite, kaolinite and alumina) gave the highest density. While boron free raw material mixture of zeolite, wollastonite, alumina, quartz gave 92,37% of relative density after sintering at 1300 °C for 1h, the same raw material composition with 1wt% of boron oxide addition gave 96, 18% of relative density at the same sintering temperature.
4. SEM results confirmed the XRD and density results. EDS studies showed that no any other phases than detected in the XRD were detected in the microstructure.

REFERENCES

- [1] Anorthite, (2008) Encyclopedia Britannica, <http://www.reference.com/browse/anorthite>(16.08.2012)
- [2] Knickerbocker,S.H., Kumar, A.H., Herron, L.W. (1993) Cordierite glass-ceramics for multilayer ceramic packaging, American Ceramic Society. Bull. 72(1), 90–95.
- [3] Lee S., Kim G. (2002) Characteristics and densification behavior of anorthite powder synthesized by a solution process employing a polymer carrier, Journal of Ceramic Process Res. 3(3), 136–140.
- [4] Mergen A., Aslanoğlu Z. (2003) Low-temperature fabrication of anorthite ceramics from kaolinite and calcium carbonate with boron oxide addition, Ceram. Int. 29(5), 667–670.
- [5] Ackley,M. ,Rege,S.U., Saxena,H. (2003) Application of natural zeolites in the purification and separation of gases, Microporous and Mesoporous Materials 61, 25-42
- [6] Ceramic, The free encyclopedia Wikipedia, <http://en.wikipedia.org/wiki/Ceramic> (05.12.2013)
- [7] What Are Ceramics? University of Illinois Materials Science and Technology Teacher's Workshop, <http://matse1.matse.illinois.edu/ceramics/ware.html> (03.12.2013)
- [8] Material Properties Charts, Ferro-Ceramic Grinding, Inc. <http://www.ceramicindustry.com/ext/resources/pdfs/2013-CCD-Material-Charts.pdf> (01.12.2013)
- [9] Ceramic, The free encyclopedia Wikipedia, http://en.wikipedia.org/wiki/Ceramic_materials (05.12.2013)
- [10] Langer, L.E. (1989) Materials and Electronic Phenomena, 103-107. http://books.google.com.tr/books?id=c2YxCCaM9RIC&pg=PA106&dq=electronic+substrates&hl=en&sa=X&ei=qHeoUqX-Gcfm7AbEgIGYDA&redir_esc=y#v=onepage&q&f=false (01.12.2013)
- [11]Chasserio,N., Guillemet-Fritsch,S., Lebey, T., Dagdag, S. (2009), Ceramic substrates for high temperature electronic integration, Journal of Electronic Materials 38(1), 164-174 http://oatao.univ-toulouse.fr/3845/1/Chasserio_3845.pdf (03.12.2013)

[12] Bhedwar, H.C., Sawhill, H.T. (1989) Ceramic Multilayer Package Fabrication, 460-470.

http://books.google.com.tr/books?id=c2YxCCaM9RIC&pg=PA460&dq=ceramic+substrate+manufacturing&hl=en&sa=X&ei=oYOoUvfHKPSS7AbejIHgDA&redir_esc=y#v=onepage&q=ceramic%20substrate%20manufacturing&f=false (03.12.2013)

[13] Ciofani, G., Menciassi, A. (2012) Piezoelectric Nanomaterials for Biomedical Applications, 35-36.

http://books.google.com.tr/books?id=PKwlrW-CrxUC&pg=PA35&lpg=PA35&dq=what+is+%22mixed+oxide+technique%22?&source=bl&ots=UV5Bo4bLqW&sig=moHL3GiNlbNUp5T44k_gwimfeec&hl=tr&sa=X&ei=RUYjUtVIkffKA9nNgYAC&ved=0CEEQ6AEwAw#v=onepage&q=what%20is%20%22mixed%20oxide%20technique%22%3F&f=false(03.12.2013)

[14] Parinov, I.A. (2012) Microstructure and Properties of High-Temperature Superconductors, 2nd Edition, Springer Heidelberg New York, New York, USA

http://books.google.com.tr/books?id=NQdHAAAAQBAJ&pg=PA139&dq=%22advantages+of+mixed+oxide+technique%22&hl=tr&sa=X&ei=WlijUqynC_OA7Qaq2IHICA&ved=0CDEQ6AEwAA#v=onepage&q=%22advantages%20of%20mixed%20oxide%20technique%22&f=false (01.12.2013)

[15] Kavalci, S., Yalamac, E, Akkurt, S. (2008) Effects of boron addition and intensive grinding on synthesis of anorthite ceramics, *Ceramics International* 34,1629–1635

[16] Baran, B., Sarıkaya, Y., Alemdaroğlu, T., Önal, M. (2003) The effect of boron containing frits on the anorthite formation temperature in kaolin–wollastonite mixtures, *Journal of the European Ceramic Society* 23, 2061–2066.

[17] Taskiran, M.U., Demirkol N., Capoglu, A. (2005) A new porcelainised stoneware material based on anorthite, *Journal of the European Ceramic Society* 25, 293-300.

[18] Marques, V.M.F., Tulyaganov, D.U., Agathopoulos, S., Ferreira, J.M.F. (2008) Low temperature production of glass ceramics in the anorthite–diopside system via sintering and crystallization of glass powder compacts, *Ceramics International* 34, 1145-1152.

[19] Traore, K., Kabre, T.S., Blanchart, P., Low temperature sintering of pottery clay from Burkina Faso, *Applied Clay Science* 17 (2000) 279-292

[20] Agathopoulos, S., Tulyaganov, D.U., Marques, P.A.A.P., Ferro, M.C., Fernandes, M.H.V., Correia, R.N. (2003) The fluorapatite–anorthite system in biomedicine, *Biomaterials* 24, 1317-1331.

[21] Mergen, A., Kayed, T.S., Bilen, M., Qasrawi, A.F., Gürü, M. (2004) Production of anorthite from kaolinite and CaCO_3 via colemanite, *Key Engineering Materials* 264–268 (4), 1475–1478.

ÖZGEÇMİŞ

Adı Soyadı : Sinem YAKICI
Doğum Yeri ve Tarihi : Bandırma, 05.03.1985
Yabancı Dili : İngilizce
E-Posta : sinemyakici@gmail.com

Öğrenim Durumu

Derece	Bölüm/Program	Üniversite/Lise	Mezuniyet Yılı
Lise	Fen Bölümü	Bandırma Anadolu Lisesi	2003
Üniversite	Metalurji ve Malzeme Müh.	Marmara Üniversitesi	2008

İş Deneyimi

Yıl	Firma/Kurum	Görevi
2010 -2012	Burçelik A.Ş.	Satış ve Teklif Mühendisi
2013 - 2013	Tat Metal Tic. ve San. Ltd. Şti.	Kalite Kontrol Mühendisi